

EXPERIMENTAL INVESTIGATION ON THE TORQUE LOSS OF AN AUTOMOBILE  
AIR CONDITIONING SYSTEM

by  
Halil Örs

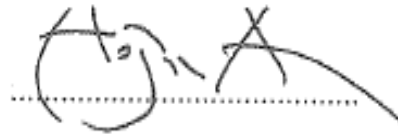
Submitted to the Institute of Graduate Studies in  
Science and Engineering in partial fulfillment of  
the requirements for the degree of  
Master of Science  
in  
Mechanical Engineering

Yeditepe University  
2013

EXPERIMENTAL INVESTIGATION ON THE TORQUE LOSS OF AN AUTOMOBILE  
AIR CONDITIONING SYSTEM

APPROVED BY:

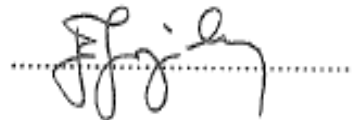
Assoc. Prof. Dr. Hojin Ahn (Erdem An)  
(Thesis Supervisor)



Prof. Dr. Oktay Özcan



Asst. Prof. Esra Sorgüven



DATE OF APPROVAL: .../.../...

## **ACKNOWLEDGEMENTS**

First of all I would like to thank my thesis supervisor Assoc. Prof. Dr. Hojin Ahn for his guidance and support during my thesis period.

I also acknowledge my family for giving great support to complete my thesis.

The Scientific and Technological Research Council of Turkey (TUBITAK) is also acknowledged for financial support during my master education.

This study is accomplished with the great support of my company Ford Otosan. So, I would like to thank my supervisor and manager for their understanding and support during my master education.

I specially acknowledge my colleague Yiğit Koyuncuoğlu who always supported me not only during my thesis studies but also whenever I need his support.

Lastly, I would like to thank my friends Efe Ünal, Burak Yegin and Asil Aksekili for their friendship.

## **ABSTRACT**

### **EXPERIMENTAL INVESTIGATION ON THE TORQUE LOSS OF AN AUTOMOBILE AIR CONDITIONING SYSTEM**

An automobile air conditioner (A/C) compressor is usually driven by an engine crankshaft, and thus the A/C system may be considered a device that consumes torque from the engine. In order not to degrade the engine performance, therefore, the torque demand by the A/C system should be predicted and compensated accurately. In the present study, the steady-state A/C compressor torque loss is investigated experimentally. The A/C system is instrumented to measure temperatures of the A/C refrigerant while the vehicle is being driven at several cruise speeds with different outside air temperatures and engine speeds (RPM). Other required data are collected from the sensors that are already implemented to the vehicle. A computer program is written to analyse the data thermodynamically, and thus the compressor torque values are obtained at various vehicle-operating conditions. Finally, the experimental result in the present study is compared with the torque loss map provided by Powertrain Control Module (PCM). The map is re-calibrated based on the present experimental results. In addition, the A/C system performance at different operating conditions is evaluated by examining the isentropic efficiency of the compressor and the coefficient of performance (COP) of the A/C system.

## ÖZET

### **BİR OTOMOBİL KLİMA SİSTEMİNİN TORK KAYBININ DENEYSEL OLARAK İNCELENMESİ**

Bir otomobil klima sisteminin kompresörü genellikle motor krank mili tarafından sürülür, bundan dolayı klima sistemi motordan tork tüketen bir cihaz olarak düşünülebilir. Motorun performansından ödün vermemek için klima sistemi tarafından talep edilen tork doğru bir şekilde tahmin edilerek telafi edilmelidir. Bu çalışmada, klima sistemi kompresörünün kararlı haldeki tork kaybı deneysel olarak incelenmiştir. Klima sistemi araç birçok farklı seyir hızında sürülürken farklı dış ortam sıcaklıklarında ve motor hızlarında klima sistemindeki soğutkanın sıcaklığını ölçmek üzere enstrümante edilmiştir. Diğer gerekli veriler araç üzerinde var olan sensörlerden toplanmıştır. Verileri termodinamik olarak analiz etmek için bir bilgisayar programı yazılmıştır ve dolayısıyla kompresörün tork kayıp verileri birçok çalışma noktasında elde edilmiştir. Son olarak, bu çalışma sonunda elde edilen deneysel sonuçlar motor kontrol ünitesi içerisinde yer alan tork kayıp haritası ile karşılaştırılmıştır. Harita deneysel sonuçlar doğrultusunda tekrar kalibre edilmiştir. Buna ek olarak, klima sisteminin farklı çalışma koşullarındaki performansı kompresörün izentropik verimi ve klima sisteminin performans katsayısı incelenerek değerlendirilmiştir.

## TABLE OF CONTENTS

ACKNOWLEDGEMENTS.....	iii
ABSTRACT.....	iv
ÖZET .....	v
TABLE OF CONTENTS.....	vi
LIST OF FIGURES .....	viii
LIST OF TABLES.....	xi
LIST OF SYMBOLS/ABBREVIATIONS.....	xiii
1. INTRODUCTION .....	1
2. BACKGROUND AND THEORY .....	4
2.1. IDEAL VAPOR-COMPRESSION REFRIGERATION CYCLES.....	6
2.2. ACTUAL VAPOR-COMPRESSION REFRIGERATION CYCLES.....	10
2.3. THE ANALYZED A/C SYSTEM.....	13
3. METHODOLOGY .....	17
3.1. DATA COLLECTION FROM VEHICLE SENSORS.....	17
3.2. A/C SYSTEM INSTRUMENTATION .....	19
3.3. DATA ACQUISITION PROCESS.....	22
3.3.1. Data Acquisition From Instrumentation Sensors .....	22
3.3.2. Data Acquisition From Vehicle Sensors .....	26
3.4. DATA PROCESSING .....	28
4. VEHICLE TEST RESULTS .....	33
4.1. PRE-CALIBRATED A/C COMPRESSOR TORQUE LOSS MAP.....	33
4.2. TEST RESULTS AT 17 °C OUTSIDE TEMPERATURE .....	34
4.3. TEST RESULTS AT 11 °C OUTSIDE TEMPERATURE .....	44
4.4. TEST RESULTS AT 21 °C OUTSIDE TEMPERATURE .....	49
4.5. TEST RESULTS AT 23 °C OUTSIDE TEMPERATURE .....	55
4.6. A/C COMPRESSOR TORQUE LOSS MAP CALIBRATION.....	61
5. CONCLUSION.....	63
6. FUTURE WORK.....	66
APPENDIX A: THE DEVELOPED MATLAB SCRIPT .....	67

REFERENCES .....	76
REFERENCES NOT CITED .....	77

## LIST OF FIGURES

Figure 2.1.	Component layout of the analyzed A/C system .....	4
Figure 2.2.	Component layout and process flow of the ideal vapour-compression refrigeration cycle.....	7
Figure 2.3.	T-s diagram of the ideal vapour-compression refrigeration cycle.....	7
Figure 2.4.	P-h diagram of the ideal vapour-compression refrigeration cycle .....	10
Figure 2.5.	Component layout and process flow of the actual vapour-compression refrigeration cycle.....	11
Figure 2.6.	T-s diagram of the actual vapour-compression refrigeration cycle.....	12
Figure 2.7.	Component layout and process flow of the analyzed A/C system[1]] ....	13
Figure 2.8.	The A/C compressor that is implemented to the analyzed A/C system [2] .....	14
Figure 3.1.	Properties of the instrumentation surface thermocouple .....	20
Figure 3.2.	The surface thermocouple along with the insulation material.....	20
Figure 3.3.	Instrumentation points on the A/C system .....	21
Figure 3.4.	The instrumentation on the evaporator inlet and outlet.....	21
Figure 3.5.	Data acquisition process from instrumentation sensors .....	22
Figure 3.6.	Illustration of the measurement setup for instrumentation channels.....	24



Figure 3.7. ATI Vision Hub [4] .....	25
Figure 3.8. Data acquisition process from PCM.....	26
Figure 3.9. Kvaser leaf cable [5].....	27
Figure 3.10. Inputs and outputs of the developed Matlab script.....	28
Figure 3.11. Bilinear interpolation.....	31
Figure 4.1. Variation of the isentropic efficiency of the compressor at average of 2038rpm engine speed and 17°C outside temperature test.....	36
Figure 4.2. Variation of the COP of the A/C system at average of 2038rpm engine speed and 17°C outside temperature test.....	37
Figure 4.3. Variation of the compressor power at average of 2038rpm engine speed and 17°C outside temperature test.....	38
Figure 4.4. Comparison of the compressor torque loss between test results and PCM output at average of 2038rpm engine speed and 17°C outside temperature test.....	39
Figure 4.5. Comparison of the compressor torque loss between test results and PCM output at average of 2505 rpm engine speed and 17°C outside temperature test.....	40
Figure 4.6. Comparison of the compressor torque loss between test results and PCM output at average of 2926 rpm engine speed and 17°C outside temperature test.....	41
Figure 4.7. Comparison of the compressor torque loss between test results and PCM output at average of 1615 rpm engine speed and 11°C outside	

temperature test.....	45
Figure 4.8. Comparison of the compressor torque loss between test results and PCM output at average of 2039 rpm engine speed and 11°C outside temperature test.....	46
Figure 4.9. Comparison of the compressor torque loss between test results and PCM output at average of 2504 rpm engine speed and 11°C outside temperature .....	47
Figure 4.10. Comparison of the compressor torque loss between test results and PCM output at average of 2064 rpm engine speed and 21°C outside temperature .....	51
Figure 4.11. Comparison of the compressor torque loss between test results and PCM output at average of 2540 rpm engine speed and 21°C outside temperature .....	52
Figure 4.12. Comparison of the compressor torque loss between test results and PCM output at average of 2968 rpm engine speed and 21°C outside temperature .....	53
Figure 4.13. Comparison of the compressor torque loss between test results and PCM output at average of 2064 rpm engine speed and 23°C outside temperature .....	56
Figure 4.14. Comparison of the compressor torque loss between test results and PCM output at average of 2537 rpm engine speed and 23°C outside temperature .....	57
Figure 4.15. Comparison of the compressor torque loss between test results and PCM output at average of 2967 rpm engine speed and 23°C outside temperature .....	58

## LIST OF TABLES

Table 3.1. Properties of the thermocouple module .....	23
Table 3.2. Properties of the ATI Vision Hub.....	25
Table 3.3. Properties of the Kvaser cable .....	27
Table 4.1. Pre-calibrated steady-state A/C compressor torque loss map.....	34
Table 4.2. Normalized average values of the temperature and pressure data of the refrigerant from 17°C outside temperature tests .....	35
Table 4.3. Normalized average values of the test results for 17°C outside temperature tests .....	42
Table 4.4. Normalized average values of the temperature and pressure data of the refrigerant from 11°C outside temperature tests.....	44
Table 4.5. Normalized average values of the test results for 11°C outside temperature tests .....	48
Table 4.6. Normalized average values of the temperature and pressure data of the refrigerant from 21°C outside temperature tests.....	49
Table 4.7. Normalized average values of the test results for 21°C outside temperature tests .....	54
Table 4.8. Normalized average values of the temperature and pressure data of the refrigerant from 23°C outside temperature tests.....	55
Table 4.9. Normalized average values of the test results for 21°C outside	

temperature tests .....	59
Table 4.10. Normalized steady-state A/C compressor torque loss map that is re-calibrated based on test results.....	61
Table A.1. The developed Matlab script that performs the thermodynamic analyses...	67

## LIST OF SYMBOLS / ABBREVIATIONS

<i>A/C</i>	Air conditioning
<i>CAN</i>	Control area network
<i>COP</i>	Coefficient of performance
<i>COP<sub>R</sub></i>	Coefficient of performance of a refrigerator
<i>EDAQ</i>	External data acquisition module
<i>HIL</i>	Hardware in the loop
<i>HS</i>	High speed
<i>PCM</i>	Powertrain control module
<i>RPM</i>	Revolution per minute
<i>USB</i>	Universal serial bus
$h_1$	Enthalpy of the refrigerant at compressor suction (kJ/kg)
$h_2$	Enthalpy of the refrigerant at compressor discharge (kJ/kg)
$h_{2s}$	Isentropic enthalpy of the refrigerant at compressor discharge (kJ/kg)
$h_3$	Enthalpy of the refrigerant at condenser outlet (kJ/kg)
$h_4$	Enthalpy of the refrigerant at evaporator inlet (kJ/kg)
$\dot{Q}_H$	Heat rejection rate to the environment (kW)
$\dot{Q}_L$	Heat absorption rate from the refrigerated space (kW)
$T$	Torque loss of the compressor (Nm)
$\dot{W}$	Work input to the compressor (W)
$\dot{W}_{net,in}$	Net work input to the compressor (W)
$\eta_c$	Isentropic efficiency of the compressor (%)

## 1. INTRODUCTION

Nowadays almost all of the automobiles are equipped with air conditioning systems to keep cabin temperature and humidity at comfortable levels in all environmental driving conditions. As a result of a significant increasing competition in the market, the performance and characteristics of the A/C system have gained more importance in order to enable customers to have more comfortable driving conditions.

It is aimed to minimize undesired effects of the A/C system on the engine performance such as compressor torque loss while keeping the temperature and humidity at desired levels in the cabin. Regarding all of these reasons, analysis of the A/C system in a thermodynamic perspective has vital importance to observe heating and cooling performance of the system as well as its effect on the engine performance in terms of torque loss.

Although the main purpose of A/C systems is the same, the component layout and types of the components vary predominantly among brands and even in one specific brand due to several reasons such as performance requirements and cost. Different systems have their own advantages and disadvantages. For instance, automatic A/C systems can control the cabin temperature set by the driver; however, this is not possible with manual A/C systems. On the other hand, manual climate systems cost less compared to automatic ones.

Most of the automobile A/C systems work based on vapour-compression refrigeration cycle and consists of four major components; a compressor, a condenser, an evaporator and a thermal expansion valve. The system requires work input to complete the refrigeration cycle and provide cooling to the cabin. The A/C compressor is the component that requires work input to compress the refrigerant and the work input to the compressor can be provided via engine crankshaft. The engine-driven A/C compressors are connected to the crankshaft via a belt; hence it is a device that consumes torque from the engine. This indicates the fact that it plays a crucial role to estimate A/C compressor torque loss in order not to degrade engine performance when the A/C system is in operation.

In the analysed application, the torque requirement of the A/C compressor is calculated inside Powertrain Control Module (PCM) as an output of a calibration map. The output of this map is used inside PCM to compensate the torque loss due to A/C compressor. In this manner, it is aimed to keep the engine performance at desired levels by compensating the torque requirement from A/C compressor when the A/C system is in operation. Thus, it is very important to calibrate the torque loss map of the A/C compressor correctly to perform accurate compensation for the additional torque requirement from A/C compressor.

This study covers the experimental investigation of steady-state torque loss of an air conditioning compressor of a commercial vehicle to calibrate the steady-state PCM torque loss map. The system is modelled as a vapour-compression refrigeration cycle with four main components including a compressor, a condenser, an evaporator and a thermal expansion valve. Thermodynamic analyses of the A/C system are performed with the temperature and pressure data obtained from vehicle tests. The vehicle tests are performed to collect temperature and pressure data from the A/C system at different ambient air temperatures and engine speeds. The A/C system is instrumented with the aim of collecting the necessary data. The required temperature and pressure data are collected from the instrumentation sensors as well the sensors that are already implemented to the vehicle. After data collection is completed, data are analyzed with a computer program using MATLAB script to calculate the compressor torque loss. The torque loss calculations for the A/C compressor from the analyses are compared with the output of the pre-calibrated steady-state torque loss map outputs and the map is re-calibrated using the results of analyses.

The calibration work is performed in Hardware in the Loop (HIL) system. HIL system simulates the vehicle as it includes the vehicle and engine models that can be controlled by PCM. This enables performing calibration work without requiring vehicle usage since PCM is present as hardware in the system. Since it is needed to control the engine speed and refrigerant pressure to calibrate the A/C torque loss map, HIL environment offers very convenient environment for re-calibrating the torque loss map based on the test results. Engine speed and refrigerant pressure are set to the values observed in the vehicle tests in the HIL rig. In this manner, compressor torque loss map is calibrated without requiring any vehicle usage.

Moreover, the isentropic efficiency of the compressor and the coefficient of performance (COP) of the A/C system at various outside air temperature and engine speed conditions are examined. The change in isentropic efficiency of the compressor and COP of the A/C system with changing engine speed and environmental temperature conditions are investigated.



## 2. BACKGROUND AND THEORY

The present study investigates a manual A/C system of a commercial vehicle. The system has been analyzed as a vapour-compression refrigeration cycle which is composed of four main components; a compressor, a condenser, an evaporator and an expansion valve. There is an electric fan located in front of the condenser to increase cooling on the condenser. Working fluid in the refrigeration cycles is called refrigerant. The present system employs R134a as a refrigerant which circulates in the A/C pipes to absorb and reject heat. The component layout of the analyzed system is shown in Figure 2.1.

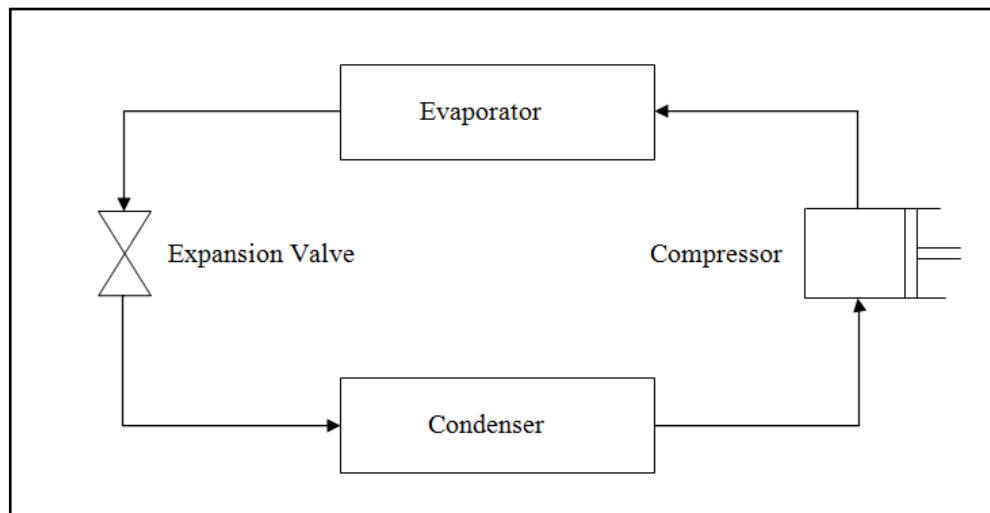


Figure 2.1. Component layout of the analyzed A/C system

In a vapour-compression refrigeration cycle, refrigerant enters the compressor as a vapour and its temperature is relatively low. The purpose of the compressor is to increase the pressure of the refrigerant. Once the pressure of the refrigerant is increased with compression process, its temperature also increases at the compressor exit. Refrigerant enters the condenser with relatively high temperature and pressure and flows through the coils of the condenser by rejecting heat to the environment. With this process, vapour refrigerant cools down and condenses in the condenser. The next step of the cycle occurs in a thermal expansion valve where the pressure and temperature of the refrigerant decrease sharply. This is the desired process before the refrigerant enters the evaporator as it should

remove heat from refrigerated space in the evaporator. As a final step of the cycle, the evaporation process in the evaporator can be considered. Once refrigerant enters the evaporator at low pressure and temperature, it can absorb heat from the refrigerated space to cool down it. The cycle is completed when the refrigerant exits the evaporator and enters the compressor again.

The purpose of a refrigeration cycle is to cool down the refrigerated space, and thus the desired output of the cycle is the absorbed heat from the refrigerated space. On the other hand, the required input to the system is the work provided to the compressor to accomplish the compression process.

The performance indicator of a refrigerator is expressed by the coefficient of performance (COP) and it is denoted as  $COP_R$ . It is defined as;

$$COP_R = \frac{\text{Desired Output}}{\text{Required Input}} = \frac{\text{Cooling Effect}}{\text{Work Input}} = \frac{Q_L}{W_{net,in}} \quad (2.1)$$

where  $Q_L$  is the amount of heat removed from the refrigerated space and  $W_{net,in}$  is the net work input to the A/C system.

The isentropic efficiency, which indicates how much compression process deviates from the isentropic compression process, is defined as;

$$\eta_c = \frac{h_{2s} - h_1}{h_2 - h_1} \quad (2.2)$$

where  $h_{2s}$  is the enthalpy of the refrigerant at compressor exit assuming the compression process is isentropic,  $h_2$  is the enthalpy of the refrigerant at compressor exit and  $h_1$  is the enthalpy of the refrigerant at compressor inlet. The isentropic efficiency of compressor can also be expressed as percentage by simply multiplying the Equation 2.2 by 100.

## 2.1. IDEAL VAPOR-COMPRESSION REFRIGERATION CYCLES

The ideal vapour-compression cycle is a good starting point to understand the theory behind the refrigeration cycles despite real cycles deviate from this cycle due to several impracticalities on the ideal systems.

The ideal vapour-compression cycle consists of the same component layout given in Figure 2.1 and it includes four processes;

- Isentropic compression in the compressor (process 1 → 2)
- Heat rejection in the condenser (process 2 → 3)
- Throttling in the thermal expansion valve (process 3 → 4)
- Heat absorption in the evaporator (process 4 → 1)

The component layout and process flow of the system and T-s diagram of the system are demonstrated in Figure 2.2 and 2.3 respectively.

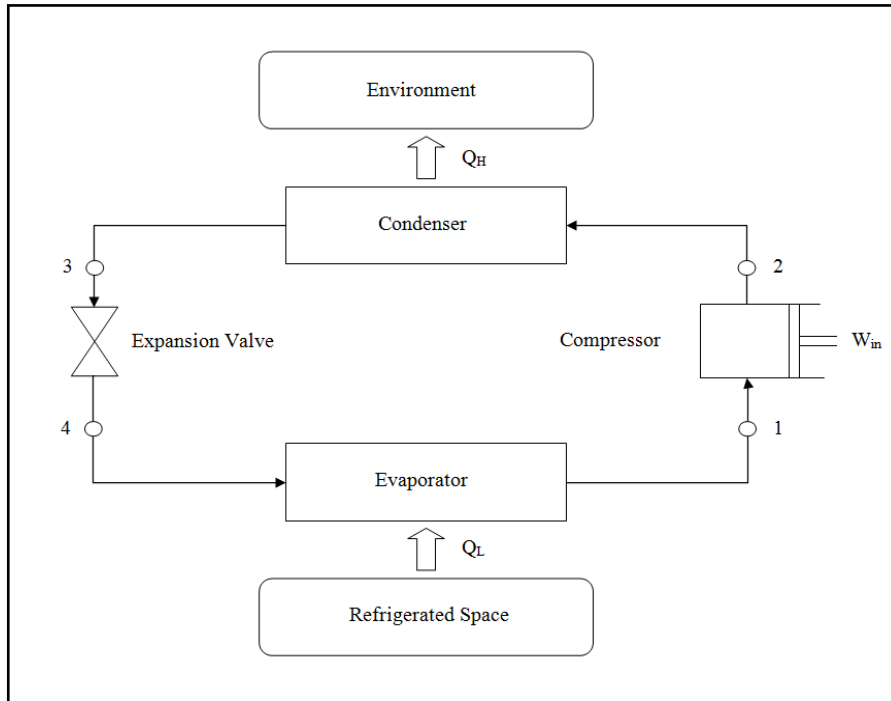


Figure 2.2. Component layout and process flow of the ideal vapour-compression refrigeration cycle

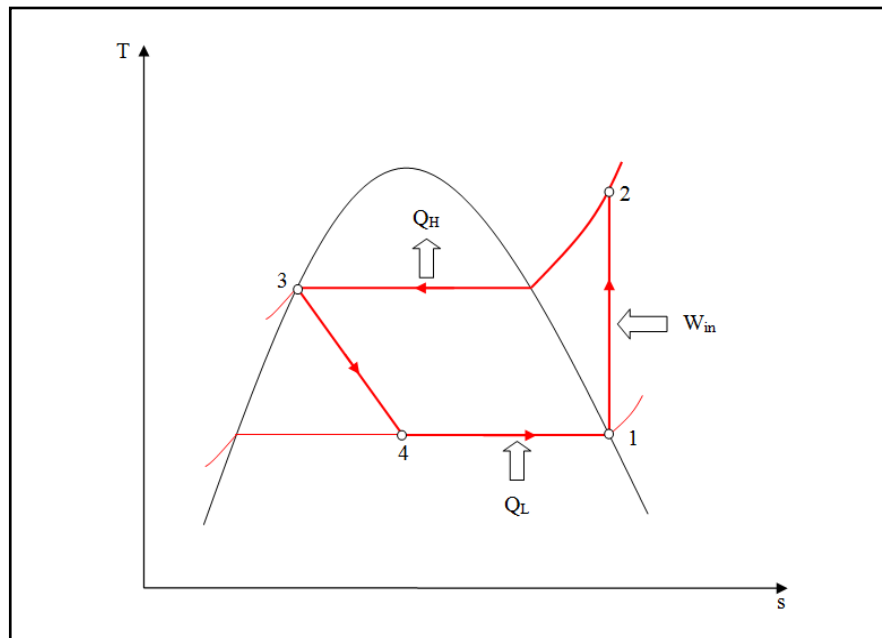


Figure 2.3. T-s diagram of the ideal vapour-compression refrigeration cycle

As is notably visible point 1 in the system shows the compressor inlet. In the ideal cycle, refrigerant enters the compressor as saturated vapour and it is compressed isentropically by the work input  $W_{in}$ . Hence, entropy of the refrigerant at compressor inlet (point 1) and compressor outlet (point 2) is shown same in Figure 3.3. When the refrigerant is compressed its temperature and pressure reaches to the levels of point 2. The work input to the compressor can be expressed as follows;

$$\dot{W} = \dot{m}(h_2 - h_1) \quad (2.3)$$

where  $\dot{m}$  stands for mass flow rate of the refrigerant and  $h_2$  and  $h_1$  denote the enthalpy of the refrigerant at compressor discharge and suction respectively.

The torque loss of the A/C compressor can be calculated from compressor power with the following expression;

$$T = \frac{30x\dot{W}}{\Pi x(\text{Compressor speed})} \quad (2.4)$$

where  $\dot{W}$  denotes the compressor power requirement calculated from Equation 2.3 and compressor speed is the angular speed of the compressor in unit of radian/s. If Watt is used as unit for  $\dot{W}$ , compressor torque loss is obtained in unit of Newton-m (Nm).

Compressor speed can be calculated simply from the following equation;

$$\text{Compressor speed} = \text{Engine speed} \times \text{Pulley ratio} \quad (2.5)$$

where pulley ratio indicates the ratio between the engine crankshaft diameter and the compressor diameter.

The refrigerant is then cooled down in the condenser by rejecting heat to the environment ( $Q_H$ ) while its pressure remains constant due to phase change process in the condenser. Refrigerant exits the condenser (point 3) as saturated liquid and enters the thermal

expansion valve. The heat rejection rate to the environment can be expressed via the following formula;

$$\dot{Q}_H = \dot{m}(h_2 - h_3) \quad (2.6)$$

where  $\dot{m}$  indicates mass flow rate of the refrigerant and  $h_2$  and  $h_3$  indicates the enthalpy of the refrigerant at condenser inlet and outlet respectively.

The refrigerant temperature decreases below the temperature of the refrigerated space when it passes through the thermal expansion valve. The refrigerant exits the expansion valve (point 4) as a saturated mixture and enters the evaporator to absorb heat from the refrigerated space ( $Q_L$ ). The rate of heat removal from the refrigerated space can be calculated as follows;

$$\dot{Q}_L = \dot{m}(h_1 - h_4) \quad (2.7)$$

where  $\dot{m}$  stands for the mass flow rate of the refrigerant and  $h_1$  and  $h_4$  indicates the enthalpy of the refrigerant at evaporator inlet and outlet respectively.

The cycle completes when the refrigerant exits the evaporator and re-enters the compressor. In this T-s diagram the area under the process curve 2-3 indicates the heat rejection to the environment and 4-1 represents the heat absorption from the refrigerated space.

The P-h diagram of an ideal vapour-compression refrigeration cycle is given in Figure 2.4. In this diagram it is easier to analyze the enthalpy change of the refrigerant with respect to pressure change throughout the system.

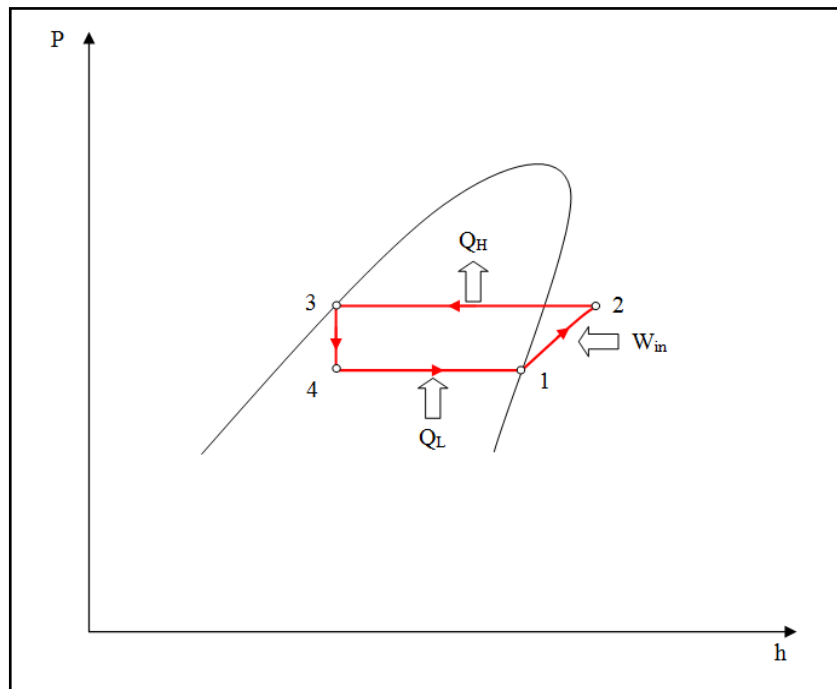


Figure 2.4. P-h diagram of the ideal vapour-compression refrigeration cycle

## 2.2. ACTUAL VAPOR-COMPRESSION REFRIGERATION CYCLES

The actual refrigeration cycles differ from ideal cycles by several reasons such as fluid friction and heat transfer to or from the system from surroundings. Figure 2.5 indicates the component layout and process flow of an actual refrigeration cycle. Compared to ideal cycles it is obvious that the component layout has same characteristics with ideal ones but the process flow requires the analysis of the refrigerant at different points from ideal ones.

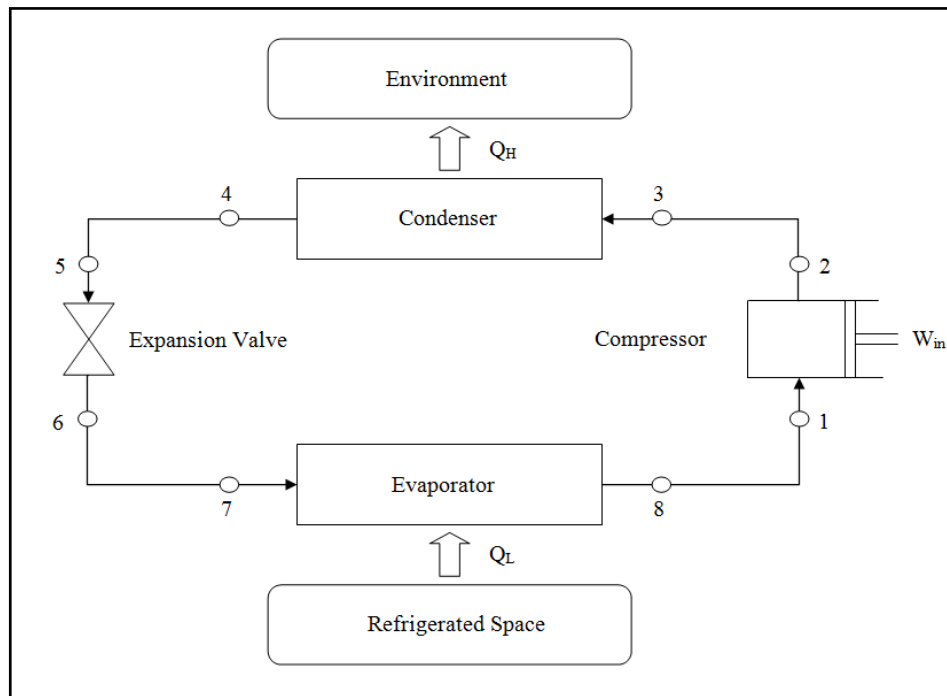


Figure 2.5. Component layout and process flow of the actual vapour-compression refrigeration cycle

The T-s diagram of an actual vapour-compression refrigeration cycle is given in Figure 2.6 in which the points are numbered based on Figure 2.5.



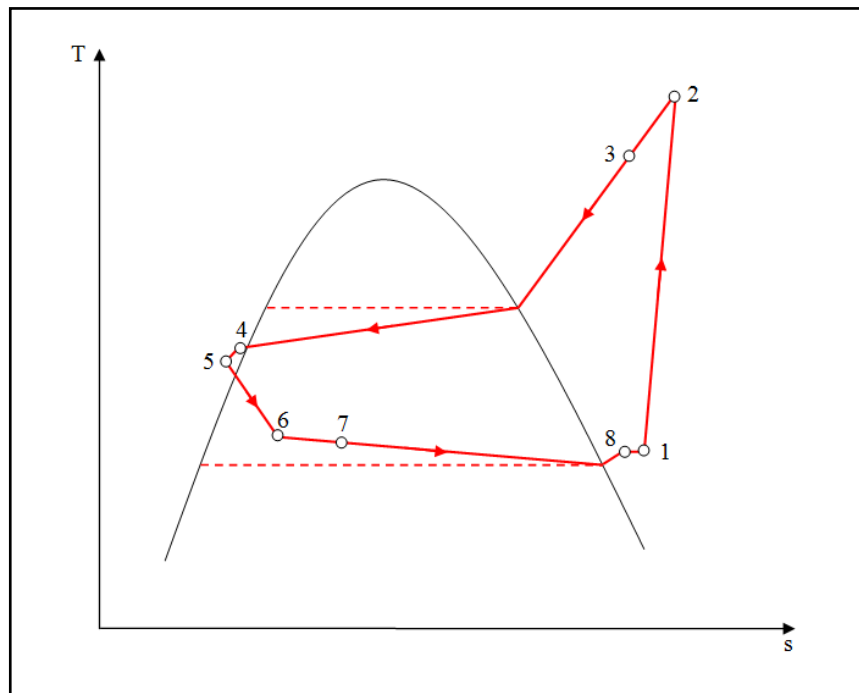


Figure 2.6. T-s diagram of the actual vapour-compression refrigeration cycle

As shown in Figure 2.6, it can be observed that the refrigerant enters the compressor as a superheated vapour instead of saturated vapour as in the ideal cycles. The system is designed like this pattern to ensure that refrigerant is completely vapoured before it enters the compressor. This is caused by the fact it may not be possible to control the state of the refrigerant so precisely.

Compression process in the actual cycle is shown as process 1→2 and it can be deduced from Figure 2.6 that this process is not isentropic. The actual compression process includes frictional effects so the entropy of the refrigerant increases from point 1 to 2 while its temperature increases as a consequence of compression process.

The actual condensing process in the condenser differs from the ideal one in terms of the state of the refrigerant at the condenser outlet. In the ideal process, the refrigerant leaves the condenser as saturated liquid but in the actual process exits the condenser as subcooled liquid due to several reasons such as pressure drop in the condenser. This situation does not constitute an issue as the refrigerant will enter the evaporator with lower enthalpy and can absorb more heat from the refrigerated space.

### 2.3. THE ANALYZED A/C SYSTEM

The analyzed system in this study is an A/C system of a commercial vehicle. The component layout of the analyzed A/C system of the vehicle is given in Figure 2.7. As shown in the figure the system consists of four main components; a compressor, a condenser, an evaporator and an expansion valve. There is an electric cooling fan located in front of the condenser which is controlled by PCM. The working fluid in the system is R134a which circulates inside A/C pipes.

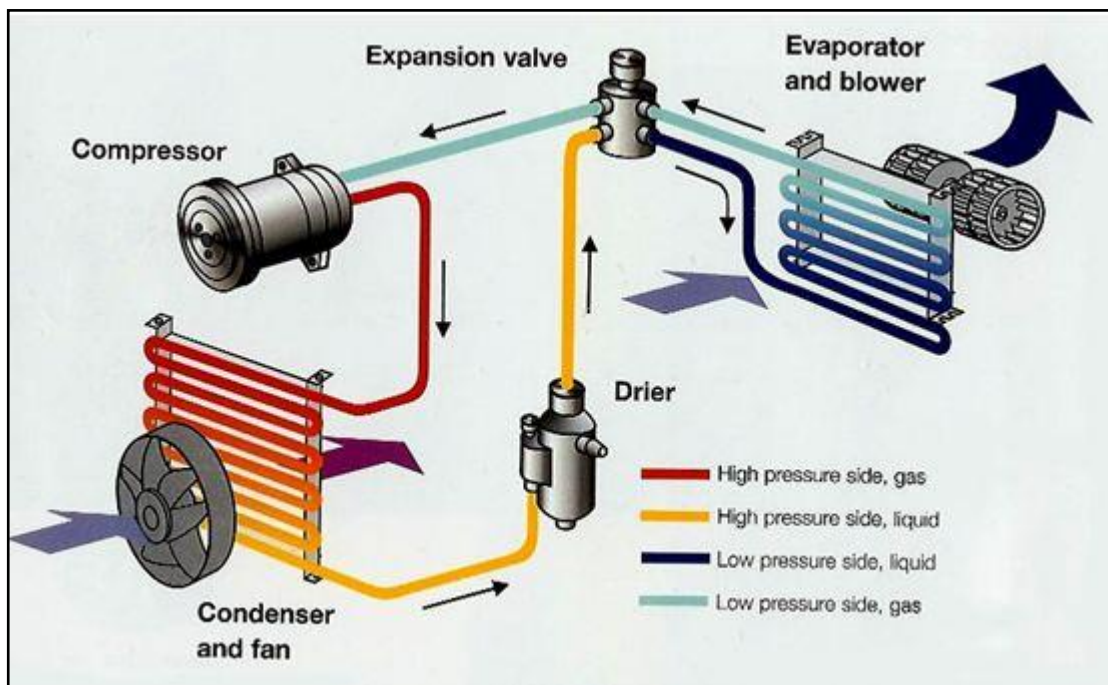


Figure 2.7. Component layout and process flow of the analyzed A/C system [1]

The A/C compressor is located in front end accessory drive (FEAD) in the engine compartment and it is connected to the engine crankshaft via belt. As a result, the compressor is driven by engine crankshaft and it consumes torque from crankshaft when it operates. The A/C compressor starts compressing the refrigerant when driver presses the A/C button on the dashboard. This signal is sent to the powertrain control module (PCM) and PCM sends this control signal to the compressor clutch. The compressor clutch is engaged after a time delay when it receives the signal from PCM and the refrigerant starts to circulate inside A/C pipes to provide cooling to the cabin. Once the A/C compressor

clutch is engaged, the compressor requires power input to compress the refrigerant. This implies that, when A/C is turned on, some part of the crankshaft torque is consumed by A/C compressor.

The A/C compressor type used in the present vehicle is the variable displacement swashplate compressor provided by Visteon. The compressor is controlled internally, meaning that there is no external control on the compressor.

The variable swashplate compressor can vary its duty cycle and change the amount of displaced refrigerant. This appropriate sizing of compressor displacement improves power consumption and fuel economy. To meet consumer demand for cabin cooling, available electronic controls provide consistent discharge air temperature, independent of drive conditions. Passengers feel more comfortable without a chance for over dehumidification [2].

Figure 2.8 shows the compressor type that is used in the analyzed A/C system.



Figure 2.8. The A/C compressor that is implemented to the analyzed A/C system [2]

The condenser in the system is located in front of the vehicle. The temperature and pressure of the refrigerant is relatively high when it exits the compressor so it is fully vapour before it enters the condenser. The refrigerant passes through the condenser coils and cools down by the convection heat transfer process. The heat rejection process takes place when the air flows through the front grill of the vehicle passes through the condenser. The refrigerant rejects heat to the environment by convection heat transfer and condenses.

There is a single electric fan located in front of the condenser to increase the amount of heat transfer from the condenser. The fan makes it sure that refrigerant is cooled down enough and condenses completely before it exits the condenser. The electric cooling fan is controlled by PCM and it is turned on when A/C compressor is engaged and starts to compress the refrigerant. The speed of the cooling fan is adjusted by PCM depending on the operating conditions of the A/C system.

The thermal expansion valve in the system provides large temperature decrease to the refrigerant. This is accomplished by adjusting the pressure of the refrigerant. No work is needed for this device to operate. The thermal expansion valve is located close to the evaporator inside the cabin. When the refrigerant passes through the expansion valve, its temperature is decreased to provide enough cooling for the evaporator.

The low temperature refrigerant enters the evaporator which is located inside the cabin. When the driver turns on the blowers on the dashboard, the air flows on the evaporator and cools down before it is blown to the cabin. The temperature of the refrigerant increases while it cools down the blown air and as a result of this process refrigerant evaporates. The cycle is completed when the low temperature gas refrigerant re-enters the compressor.

The system operates as a vapour-compression refrigeration cycle so it is modelled as an actual vapour-compression refrigeration cycle. As represented in Figure 2.8, the refrigerant enters the compressor as low pressure vapour and it is compressed to increase its pressure before it enters the evaporator. Evaporator cools down the refrigerant by rejecting heat to the environment. The refrigerant changes its state to liquid from gas as a consequence of the condensing process. The refrigerant enters the thermal expansion valve before it enters the evaporator. The thermal expansion valve enables drastic temperature decrease to the refrigerant in order to absorb heat from the evaporator region. The evaporator is located inside the cabin so refrigerant absorbs heat from the cabin while it passes through the evaporator. The temperature of the refrigerant increases during this process so the refrigerant changes state from low pressure liquid to gas as a result of evaporation process. The refrigerant re-enters the compressor as a low pressure gas and the cycle is completed with this process. The refrigerated space in this process is the cabin itself and heat is rejected from the condenser to the environment directly.

As indicated previously, A/C compressor is driven by engine crankshaft itself and consumes torque when A/C system is turned on. Although the primary purpose of the A/C system is to provide comfort to the driver in terms of cooling and humidity, it is desired to keep the vehicle performance at desired levels when A/C compressor needs additional torque from the crankshaft. Therefore it is needed to compensate the torque loss caused by A/C compressor not to degrade the vehicle performance. This task is accomplished by PCM which calculates all setpoints related with engine torque production at specific operating point. A/C torque loss is calculated inside PCM by a calibration map. The output of this map is then used to compensate the torque loss caused by the compressor. So, it has vital importance to calibrate this map correctly for vehicle performance. If the compressor torque loss is not compensated correctly, vehicle performance will be affected significantly. This performance degradation can easily be observed by the driver and this constitutes customer dissatisfaction.

To find the compressor torque requirement and analyze the A/C system performance at different operating points, it is needed to find the enthalpy values of the refrigerant at different points in the system. Since this system is modelled as an actual vapour-compression cycle, it is needed to obtain temperature and pressure information of the refrigerant at each point shown in Figure 3.6. The temperature and pressure data are collected from vehicle tests at different operating points of the compressor. The detailed information on data collection procedure and vehicle tests is given in the following sections. With these data available, the required thermodynamic analyses are performed to obtain the compressor torque loss, the isentropic efficiency and the coefficient of performance of the A/C system.

### **3. METHODOLOGY**

In this section, data collection processes from the vehicle and instrumentation sensors as well as the A/C system instrumentation procedure are given. The last part of the study introduces the method of processing the collected data.

#### **3.1. DATA COLLECTION FROM VEHICLE SENSORS**

Some of the required data to perform thermodynamic analyses of the A/C system can be collected from the sensors / switches that are already implemented to the vehicle. The following data are collected from the vehicle sensors / switches via Powertrain Control Module (PCM);

- Refrigerant pressure at compressor discharge
- Evaporator fin temperature
- Environmental temperature
- Environmental pressure
- Engine speed
- Vehicle speed
- Cooling fan low / high speed relay status
- Air conditioning clutch relay status

While some of these sensors / switches are hardwired to the PCM pins, the others communicate with PCM via high speed control area network (HS -CAN). So these entire sensor/switch data are collected from PCM.

The vehicle is equipped with an analogue refrigerant pressure sensor to monitor the air conditioning refrigerant pressure at compressor discharge throughout the usage of the vehicle. Analogue pressure information from this sensor is used along with the compressor discharge temperature to find the thermodynamic properties of the refrigerant at compressor discharge.

Evaporator in-fin temperature sensor also fitted to the vehicle and this sensor measures the temperature of the air around the middle of the evaporator. Originally, the signal from this sensor is used to control the compressor operation at any instant to be able to reach evaporator temperature setpoint. In this study, the signal from this sensor is mainly used to cross-check the temperature measurements of the surface thermocouple at evaporator inlet and evaporator outlet.

Since vehicle tests are run in outdoor, environmental temperature is the parameter that cannot be controlled throughout the vehicle tests. Ambient temperature at the time of the tests has direct effect on the thermal load on the evaporator and this has an effect on the refrigerant pressure throughout the A/C line. Thus, it is important to have ambient air measurement data in the tests.

A/C compressor torque loss and the mass flow rate of the refrigerant are function of compressor speed. So, compressor speed must be known throughout the vehicle tests. Since A/C compressor is driven by engine itself via a pulley, compressor speed is directly proportional to engine speed. Thus, engine speed is measured to calculate the compressor speed for the analyses.

Vehicle speed is another variable that has influence on the A/C system performance. As vehicle speed changes, it affects convection heat transfer from the condenser. Since vehicle tests are performed at different vehicle speeds, it is important to record the vehicle speeds during the tests. Moreover, steady-state test data are collected at constant engine speeds. The engine speed is controlled by with driving the vehicle at constant vehicle speed at a specific gear. So, it is important to monitor the vehicle speed throughout all the tests.

A single electric cooling fan placed in front of the condenser and radiator that is activated based on cooling demand from A/C system. The fan is controlled by PCM itself. It can work at two different speeds based on cooling demand level from A/C system. Activation of this fan either at low or high speed affects the air flow over the condenser. Thus, cooling fan directly affects refrigerant temperature and pressure inside A/C system. Cooling fan relay status data are collected to observe activation and speed level of the cooling fan at the instant of vehicle tests.

Air conditioner compressor clutch engagement / disengagement status can be observed and controlled by powertrain control module (PCM). Since compressor clutch can be disengaged by PCM due to several reasons such as evaporator temperature and refrigerant pressure to protect the A/C system, it is important to be sure that compressor is active and consuming torque throughout vehicle tests.

It is noticed that this much data are not enough to be able to perform thermodynamic analyses of the A/C system. Thus, additional sensors are placed to the A/C system to collect other required temperature data from the A/C system. The details of the instrumentation process are given in the next section.

### **3.2. A/C SYSTEM INSTRUMENTATION**

The on-board vehicle sensor / switch data are not sufficient to find out the thermodynamic properties of the refrigerant at required points in the system. So, the A/C system is instrumented with thermocouples to collect temperature data for the refrigerant.

The A/C system is instrumented by placing surface thermocouples onto the aluminium pipes at various locations to collect required temperature data. These data are used to perform the analysis with additional data that are provided by the sensors / switches that are already implemented to the vehicle. The required data other than instrumentation signals are obtained from power train control module (PCM) which collects and uses these signals in normal operation of the vehicle.

K-Type surface thermocouples are used to collect temperature data from the measurement points. Figure 3.1 illustrates the dimensions and the maximum operation temperature of the thermocouple.



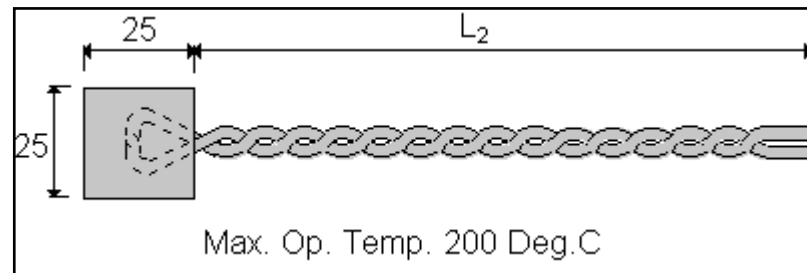


Figure 3.1. Properties of the instrumentation surface thermocouple

After placing thermocouples onto the tubes, the sensors are covered with an insulation material and tie straps are used to hold them in place. The insulation is required to get more accurate data as pipes of the A/C system is under the hood and the measurements can be easily affected from engine temperature and other noise factors from under hood environment. Figure 3.2 shows the thermocouple and the insulation material together.

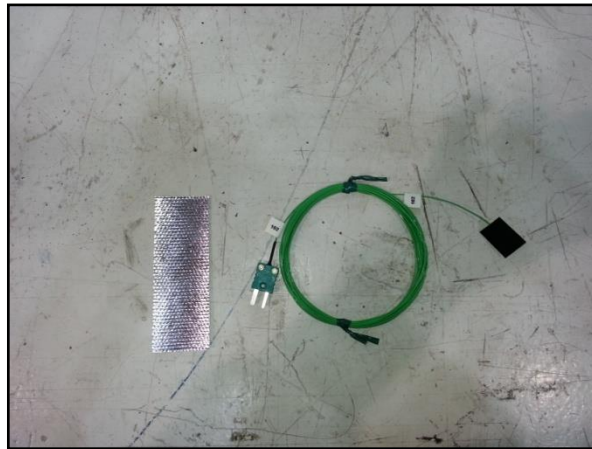


Figure 3.2. The surface thermocouple along with the insulation material

Instrumentation thermocouples are placed onto the following points in the system;

- Compressor suction – Point 1
- Compressor discharge - Point 2
- Condenser outlet - Point 3
- Evaporator inlet - Point 4
- Evaporator outlet - Point 5

- Blowers in the cabin

The schematic of the A/C system as well as the instrumentation points on the A/C system are given in Figure 3.3.

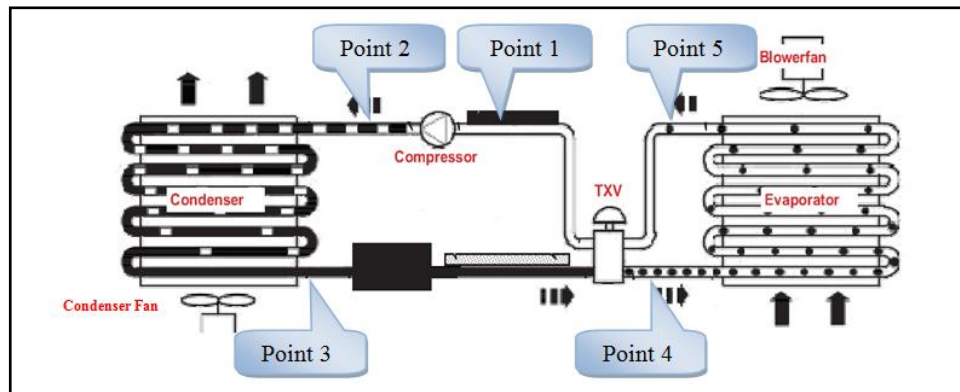


Figure 3.3. Instrumentation points on the A/C system

Evaporator inlet and outlet points are shown as point 4 and point 5 in Figure 3.3. The illustration of the evaporator inlet and outlet instrumentation is given in Figure 3.4.



Figure 3.4. The instrumentation on the evaporator inlet and outlet

It can be observed from Figure 3.4 that the thermocouples are wrapped with the insulation material and tie straps are used to fasten the thermocouple and the insulation material to the measurement point.

### 3.3. DATA ACQUISITION PROCESS

Data from PCM sensor / switches and instrumentation channels are collected via ATI Vision software. Instrumentation channels and vehicle sensors require different measurement setups to collect data.

#### 3.3.1. Data acquisition from instrumentation sensors

Instrumentation sensors on the A/C system are connected to a thermocouple module via a breakout box and this module is connected to a data acquisition device, ATI Vision Hub with an analogue input module. Vision Hub is connected to a computer with Universal Serial Bus (USB) connection. Sensor data are read from the thermocouple module and sent to a computer via ATI Vision hub data logger. Data acquisition process from the sensors to the ATI Vision software is as follows;

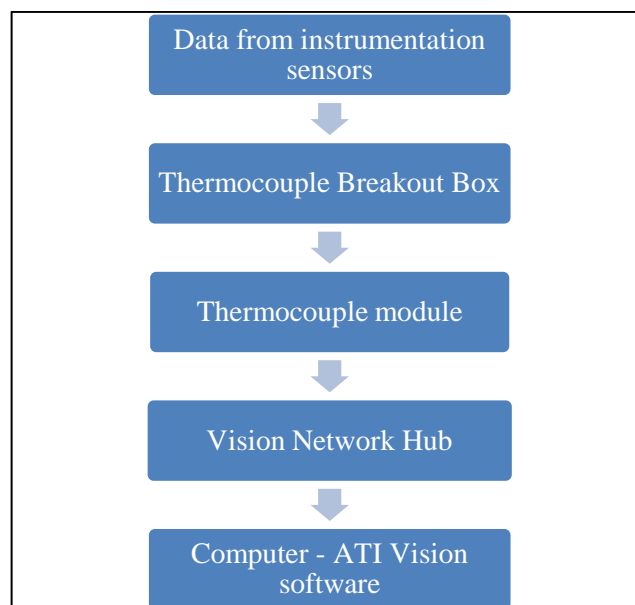


Figure 3.5. Data acquisition process from instrumentation sensors

ATI external data acquisition modules (EDAQ) are necessary for collecting and interpreting data for post analysis. These modules communicate to the ATI data acquisition software through the Network Hub on a CAN bus at 1Mb. Each is equipped with a 32-bit microprocessor, on-board flash memory and high-quality interconnects. Each analogue and thermocouple channel provides a software programmable independent acquisition rate and low-pass filter while the counter functions for the pulse counter are programmable for period and frequency measurement [3].

As indicated previously, thermocouple module is used to collect temperature readings from the sensors. The properties of this module are given in Table 3.1.

Table 3.1. Properties of the thermocouple module

Thermocouple type	J, K, T on a channel by channel basis
Thermocouple accuracy	2°C
Cold-junction accuracy	± 0.5 °C (-40°C to +85°C)
Channel to channel isolation	120 dB
Measurement speed	4 Hz per channel with 8x over-sampling

Figure 3.6 shows the measurement setup including thermocouple breakout box and thermocouple module that is used to collect temperature data from the instrumentation sensors.



Figure 3.6. Illustration of the measurement setup for instrumentation channels

The ATI Vision Network Hub is the main interface to the ATI Vision software for CAN and K-Line interfaces. It enables synchronous CAN communication from your ATI VISION system to ATI data acquisition and other vehicle interface products. It communicates to computer via (USB) connection on the Hub. The properties of the Vision Hub are given in Table 3.2 and Figure 3.7 shows the picture of the hub.

Table 3.2. Properties of the ATI Vision Hub

Configuration	Application interface	VISION Calibration and Data Acquisition Software
Indicators	LEDs	
Indicators	Switches	(2) Bus Termination
Special Capabilities	Vehicle Network Aux I/O	15-pin Dsub (provides access to VNI2/VNI2+ I/O)
Operating Conditions	Communication	High-speed ICP CAN
	Connectors	To PC: 1 USB connection To VISION hardware: 2 B Series 5-pin LEMO DC Power
	Power Supply	9 to 32 VDC
	Power Consumption	4W (with VNI2 Card)
	Temperature Range	-40°C to +85 ° C
Mechanical	Dimensions	135mm x 93mm x 29mm
	Weight	369g



Figure 3.7. ATI Vision Hub [4]

### 3.3.2. Data acquisition from vehicle sensors

Signals from PCM are collected in a different way compared to instrumentation signal data acquisition. PCM collects some of the required sensor signals via hardwired connection and some of the signals are sent via HS-CAN to the PCM.

A 2-pin LEMO and Kvaser cables are used together to be able to connect to the PCM to collect required data. LEMO cable is connected to the LEMO extension of the PCM and Kvaser cable provides connection between LEMO and computer. The signals from PCM are also collected with ATI Vision software together with instrumentation signals simultaneously. Data collection process from PCM is summarized below;

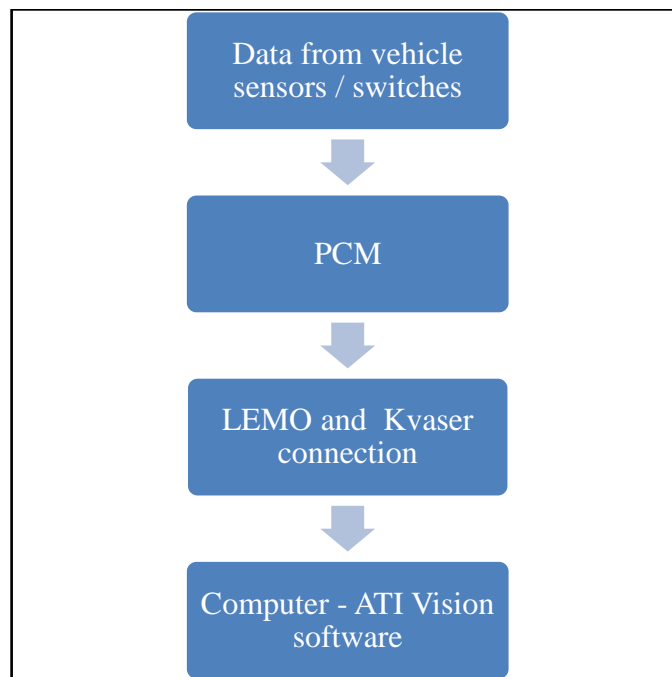


Figure 3.8. Data acquisition process from PCM

As implied in the previous stages, Kvaser cable provides USB interface for PCM signals. One side of it has 9-pin connection to the LEMO cable and other side provides USB interface to the computer. Figure 3.9 illustrates the Kvaser cable and Table 3.3 gives the technical properties of it.



Figure 3.9. Kvaser leaf cable [5]

Table 3.3. Properties of the Kvaser cable

Galvanic Isolation	No
Bitrate	5 – 1000 kbit/s
Error Frame Generation	No
Error Frame Detection	Yes
Weight	100 g
Timestamp Resolution	100 $\mu$ s
On Board Buffer	Yes
Maximum Message Rate, Send	8000
Maximum Message Rate, Receive	8000
Sound	No
Dimensions ( WxLxH)	25x100x20 mm
Temperature Range	-20°C - +75°C



### 3.4. DATA PROCESSING

MATLAB script is developed to enable collected data from the vehicle tests to be processed. The script basically takes the collected data from the vehicle tests as input and gives required outputs such as A/C compressor power input and torque loss, isentropic efficiency of the compressor, coefficient of performance (COP), heat removed from the refrigerated space and heat rejection to the environment. Figure 3.10 shows inputs and outputs of the developed script.

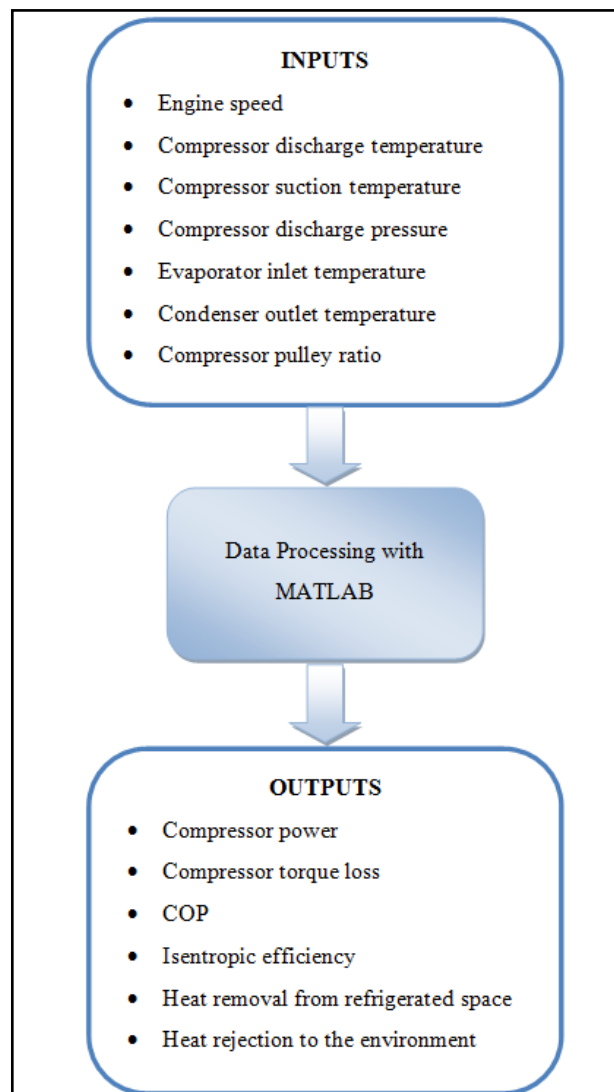


Figure 3.10. Inputs and outputs of the developed Matlab script

First step of the script generation work starts with converting vehicle test data to suitable format that can be processed with MATLAB. ATI Vision software records the data as .rec file format so it is needed to convert these files to .mat files to be able to use them in the script. These files include all the input data that are needed to obtain desired outputs.

The next step of the data processing is to perform thermodynamic analysis of the A/C system. It is required to obtain enthalpies and entropies at each point in the system. Since mass flow rate of the refrigerant mainly depends on the suction pressure and compressor speed, a separate function is created to calculate mass flow rate of the refrigerant at the time of operation. Once mass flow rates and enthalpies are known at each point in the system, compressor power and all other desired outputs can be easily calculated.

Test data are handled in the function *Read\_TestData\_To\_Mat* function. This function gets the values of the required signals from vehicle tests and outputs compressor discharge and suction pressure, evaporator inlet, evaporator fin, condenser outlet, compressor suction and discharge temperatures and engine speed. All these values except compressor suction pressure values are read from vehicle or instrumentation sensors. It is assumed that refrigerant pressure from evaporator inlet to the compressor suction is approximately same due to phase change process, so compressor suction pressure is approximated as saturation pressure of the refrigerant at evaporator inlet.

The program contains other sub-functions to calculate saturated and superheated thermodynamic properties of R134a from the thermodynamic tables. Since refrigerant may be either saturated or superheated at different points in the A/C system, it is needed to find saturated and superheated thermodynamic properties of R134a. For this purpose two different functions are generated to calculate saturated and superheated properties of the refrigerant. Thermodynamic properties of the R134a are obtained from Reference [ ] for saturated and superheated conditions. Saturated and superheated properties are read from Excel sheets and converted to .mat files with another sub-function to be able to use in the script for calculating saturated and superheated properties of the refrigerant.

The saturated properties of R134a are given as a function of the temperature of the refrigerant in thermodynamic table. Thus, it is enough to know the temperature of the

saturated refrigerant to calculate the enthalpy, entropy and other thermodynamic properties. The function *saturated\_properties* takes temperature of the refrigerant as an input and outputs saturation temperature, enthalpy, entropy and other thermodynamic properties of the saturated R134a. Saturated properties of the refrigerant can be calculated for maximum of 100°C with this function. The condition for saturation is checked in the main function *AC\_Cycle* which will be introduced at the end of the section. If the condition for saturation is satisfied the program runs the sub-function for saturated properties and gives the required outputs. Since the thermodynamic tables give the properties of the refrigerant at specific temperature points, the function performs linear interpolation when the input temperature from the test data is not available in the temperature points provided by the saturation properties table.

The superheated properties of R134a depend on both temperature and pressure. Thus, it is needed to know both temperature and pressure of the refrigerant to calculate the thermodynamic properties of it. The properties of the superheated refrigerant are calculated with *superheated\_properties* sub-function. This function enables to find the thermodynamic properties of R134a from 100kPa to 3000kPa pressure range. The properties are available for maximum temperature of 120°C. This sub-function gets refrigerant temperature and pressure as input from the vehicle test data and outputs refrigerant enthalpy, entropy and specific volume for superheated states. When the temperature and pressure data from the vehicle tests are not available at the points in the properties table, interpolation is performed both for temperature and pressure. This brings to the necessity perform bilinear interpolation. This task is performed with another sub-function.

Bilinear interpolation is performed with the function *bi\_linear\_interp*. This function finds the properties of the refrigerant when it is necessary to perform interpolation in two dimensions such as temperature and pressure. The inputs of this function are obtained by finding the nearest lower and upper values for the interpolation variables and properties at these four points. Required calculations are performed and desired properties are found as output. Figure 3.11 and Equation 3.1 are introduces how bilinear interpolation is implemented to the script.

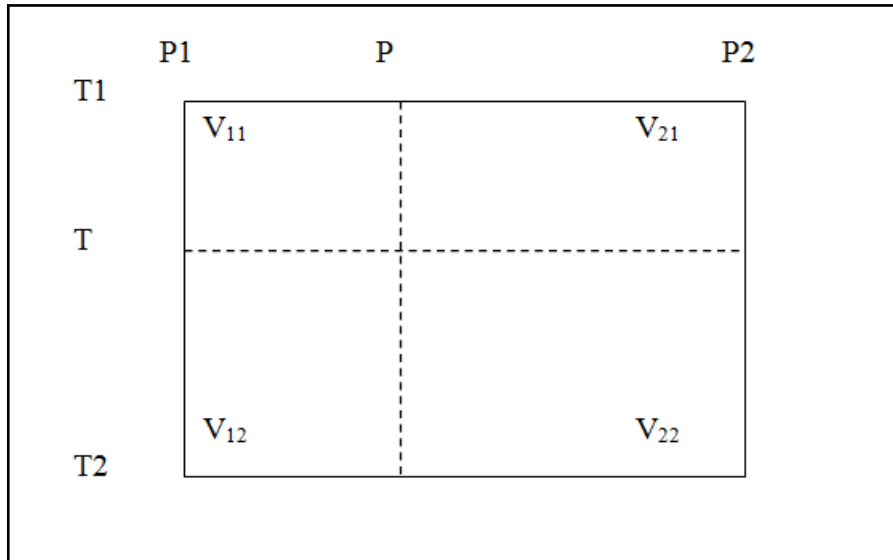


Figure 3.11. Bilinear interpolation

$$V(T, P) = \left[ \frac{T-T_1}{T_2-T_1} (V_{12} - V_{11}) + V_{11} \right] \left[ 1 - \frac{P-P_1}{P_2-P_1} \right] + \left[ \frac{T-T_1}{T_2-T_1} (V_{22} - V_{21}) + V_{21} \right] \left[ \frac{P-P_1}{P_2-P_1} \right] \quad (3.1)$$

In order to find isentropic efficiency of the compressor, it is needed to find enthalpy of the refrigerant at compressor discharge by treating compression process as isentropic. The function called *isentropic\_enthalpy* calculates isentropic enthalpy of the refrigerant at compressor exit. The input of this function is pressure and entropy and the output is isentropic enthalpy of the refrigerant at compressor discharge.

The function *mass\_flow\_rate* calculates the mass flow rate of the refrigerant from the data provided by the compressor supplier. The mass flow rate is given as a function of the compressor speed and suction pressure, and the data are available for 2 different compressor suction pressures and 6 different compressor speeds. Therefore, the present study employs a bilinear interpolation to calculate the mass flow rate from the data provided by the supplier.

The outputs of the above functions are used in the function *AC\_Cycle* to perform required calculations to find compressor work and torque loss, heat rejection to the environment, heat removal from refrigerated space, isentropic efficiency of the compressor and COP. This task is accomplished by performing thermodynamic analysis for the system. Mass

flow rate, enthalpy and entropy values of the refrigerant at compressor suction, compressor discharge, condenser outlet and evaporator inlet are used for these calculations that are calculated with the aid of the sub-functions introduced previously.

The developed Matlab scripts are introduced in Appendix A.

## **4. VEHICLE TEST RESULTS**

The vehicle tests are performed at different outside air temperatures and compressor speeds. Temperature and pressure data are collected from instrumentation and vehicle sensors and these data are processed with the developed MATLAB scripts to obtain compressor power requirement and torque loss, isentropic efficiency of the compressor and coefficient of performance (COP) of the A/C system. The torque loss outputs of the vehicle tests are compared with the pre-calibrated A/C torque loss map output and the map is re-calibrated based on the test results.

The tests are performed in the motorway at different engine speeds and outside air temperatures. In this manner, it is aimed to work on different regions of the calibration map in the tests as the axes of this map depend on the engine speed and the refrigerant pressure. All of the tests are performed by setting the maximum cooling level for A/C and setting the blower level to 1. The data collection rate from the sensors is 500 milliseconds in all of the tests. To be able to collect steady-state data, cruise control is used to drive the vehicle at constant speed at a specific gear. So, data are collected at almost constant engine speed points during the tests period.

### **4.1. PRE-CALIBRATED A/C COMPRESSOR TORQUE LOSS MAP**

The steady-state torque loss calibration map of the A/C compressor that is used during the vehicle tests is given in Table 4.1. It should be noted that the axes of the map are normalized by their maximum values. The X axis of this map depends on engine speed and the refrigerant pressure at compressor discharge and the Y axis of the map depends on the engine speed. The output of the map is compressor torque loss. The output of this map is used as steady-state compressor torque loss and it is used to compensate additional torque loss required by the A/C compressor from the engine.

Table 4.1. Normalized pre-calibrated steady-state A/C compressor torque loss map

Y \ X	0.076	0.160	0.280	0.520	0.716	1.000
0.182	0.139	0.208	0.361	0.639	0.833	1.000
0.545	0.200	0.278	0.611	0.972	1.000	1.000
0.727	0.267	0.439	0.833	1.000	1.000	1.000
1.000	0.333	0.572	0.933	0.933	0.933	0.933

When Table 4.1 is examined, it is observed that the map has 6 points in X axis and 4 points in Y axis. Depending on the operating point of the compressor, the torque loss of the A/C compressor is calculated inside PCM with this map. The map is calibrated with the reference of previous projects so it is needed to re-calibrate it specific to the current vehicle. The output of this map is compared to the test results and the some regions of the map are re-calibrated.

#### **4.2. TEST RESULTS AT 17 °C OUTSIDE TEMPERATURE**

The first test is performed when ambient air temperature is approximately 17°C. In this test, data are collected at 3 different vehicle speeds at third gear. This ends up with three different engine speed data at 17°C ambient temperature. The average values of the engine speed points for these tests are 2038 rpm, 2505 rpm and 2926 rpm. Each test is performed by driving the vehicle at constant vehicle speed approximately 10 minutes to ensure the A/C system reaches steady-state conditions in terms of temperature and pressure. Test results are plotted in terms of normalized variables by dividing each variable by its maximum value that is obtained among all vehicle test results. For example, the isentropic efficiencies of the compressor are plotted by dividing the maximum isentropic efficiency value obtained from the tests results. Thus the maximum values in the plots and tables are observed as 1.

Table 4.2 illustrates the average values of the temperature and pressure data of the refrigerant R134a that are collected from vehicle tests as well as the engine speed in unit base.

Table 4.2. Normalized average values of the temperature and pressure data of the refrigerant from 17°C outside temperature tests

Normalized Engine Speed	0.67	0.83	0.97
Normalized Discharge Pressure	0.83	0.83	0.83
Normalized Compressor Outlet Temperature	0.65	0.83	0.94
Normalized Evaporator Inlet Temperature	0.02	0.03	0.03
Normalized Evaporator Outlet Temperature	0.04	0.05	0.05

The test results show that pressure of the refrigerant at compressor discharge is nearly constant although engine speed changes. It can be observed from the results that the refrigerant temperature at compressor discharge is strongly dependent on the engine speed as compressor discharge temperature increases systematically when engine speed increases. When the refrigerant temperatures at evaporator inlet and outlet are compared with the compressor outlet temperature, it is apparent that evaporator temperatures are very low compared to compressor discharge temperature. This is an expected result since the refrigerant temperature decreases drastically due to throttling process at thermal expansion valve before it enters the evaporator. It can be also concluded from the test results that the temperature of the refrigerant at evaporator outlet is slightly higher than the refrigerant temperature at evaporator inlet. This is because the refrigerant becomes superheated at the evaporator outlet as it absorbs heat from the refrigerated space which in this case is the cabin.

The test results are analysed with MATLAB script to obtain the COP of the A/C system, the isentropic efficiency of the compressor, compressor power and torque loss values. The script also calculates the compressor suction pressure based on the temperature of the refrigerant at evaporator inlet. It is believed that the refrigerant pressure is nearly constant from the evaporator inlet to the outlet. Since the state of the evaporator inlet must be two-phase, the evaporator inlet pressure is obtained as the saturation pressure of the evaporator inlet temperature. Therefore, the compressor suction pressure is obtained as the saturation pressure of the refrigerant at evaporator inlet temperature.



The present analysis employs the mass flow rate of the refrigerant provided by the compressor supplier, which is given as a function of the compressor speed and the compressor suction pressure.

Figure 4.1 through 4.4 shows the steady-state results of the isentropic efficiency of the compressor, COP of the A/C system, compressor power input and compressor torque loss comparison between the test results and PCM outputs for 2038 rpm engine speed point.

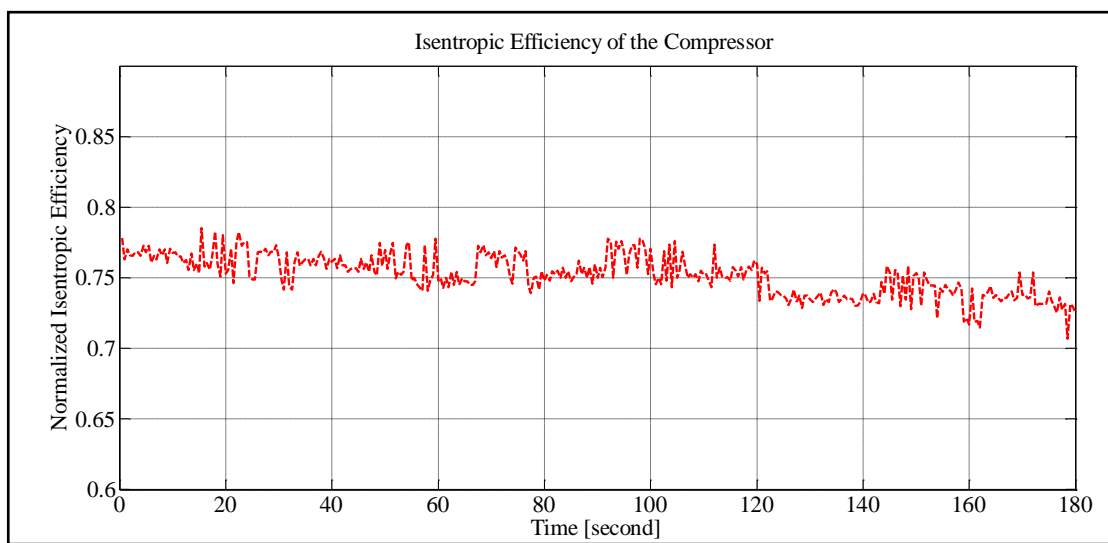


Figure 4.1. Variation of the isentropic efficiency of the compressor at average of 2038rpm engine speed and 17°C outside temperature test

When Figure 4.1 is examined, it can be observed that the normalized isentropic efficiency of the compressor is around 0.75. The variation of the isentropic efficiency during 180 seconds period is due to the fact that compressor discharge temperature changes slightly during the test period. Since the isentropic efficiency of the compressor is calculated based on Equation 2.2, it depends on the enthalpy of the refrigerant at compressor inlet and outlet. So, the change in compressor discharge temperature causes isentropic efficiency to change accordingly. The slight decrease in the isentropic efficiency is due to the fact that the temperature of the refrigerant at compressor discharge and thus the enthalpy of the refrigerant increases slightly during the period of 180 seconds while the temperature and enthalpy of the refrigerant at the compressor suction remains nearly constant during this period.

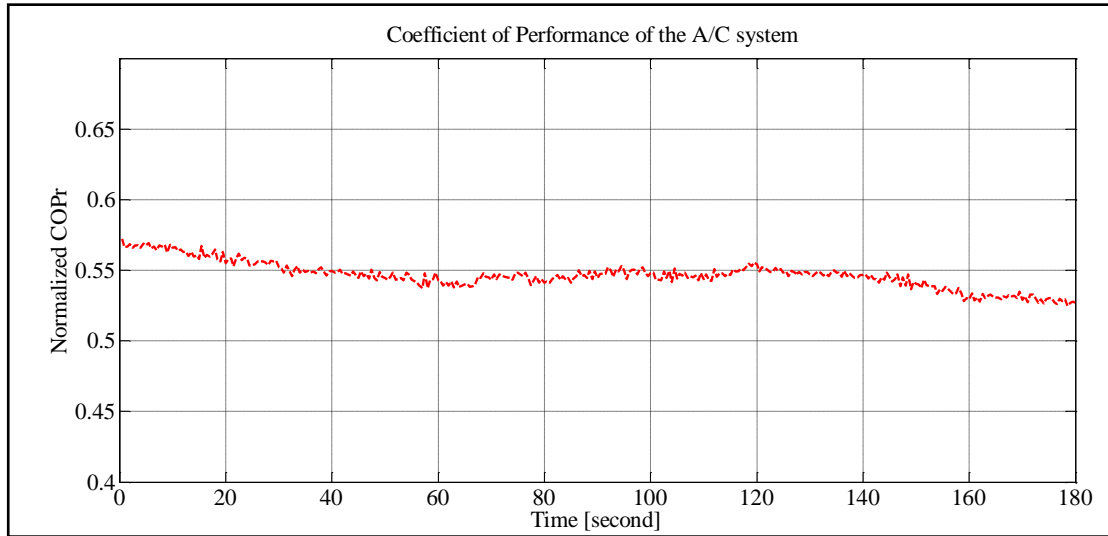


Figure 4.2. Variation of the COP of the A/C system at average of 2038rpm engine speed and 17°C outside temperature test

Figure 4.2 shows the coefficient of performance (COP) of the A/C system for average engine speed of 2038 rpm. The COP is calculated from Equation 2.1. The COP of the system for this test condition is around 0.55 although it appears that COP decreases slightly during the test period as in the case of the isentropic efficiency. COP is the ratio of desired cooling rate from the cabin to the required power input to the compressor, and it depends on the refrigerant enthalpy changes between evaporator inlet and outlet and between compressor suction and discharge. Since the refrigerant enthalpy is almost constant at evaporator inlet and exit and compressor suction, the main reason for COP decrease is believed to be caused by increase in the enthalpy of the refrigerant at compressor exit as the temperature of the refrigerant increases slightly at compressor exit as stated previously.

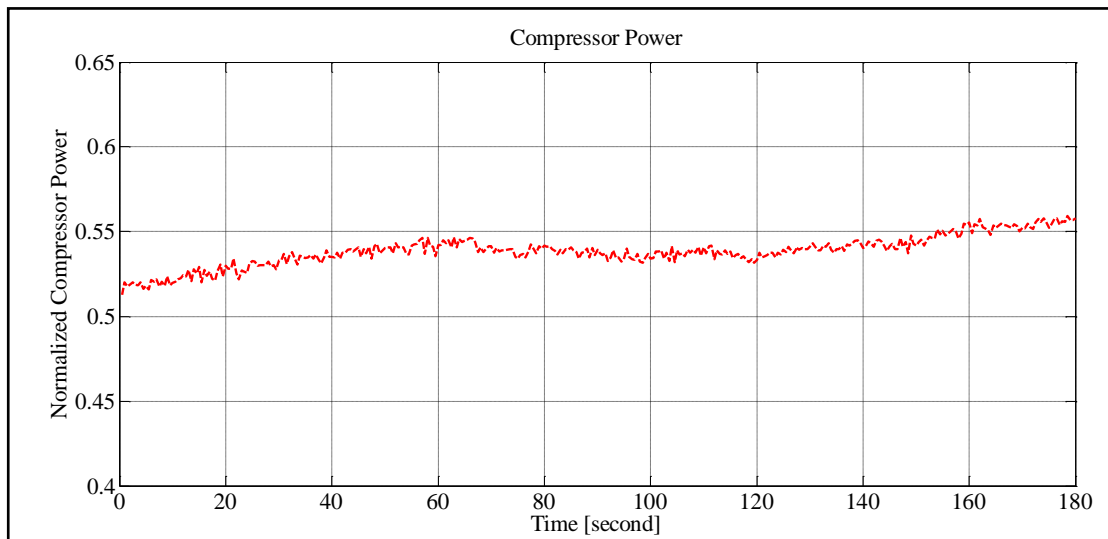


Figure 4.3. Variation of the compressor power at average of 2038rpm engine speed and 17°C outside temperature test

Figure 4.3 shows the change in compressor power during the test period. It can be observed that compressor power requirement is approximately 0.54 although it increases slightly from the beginning of the 180 seconds time period. The compressor power is calculated from the enthalpies of the refrigerant at compressor suction and discharge and the mass flow rate of the refrigerant. The compressor suction pressure, the engine speed and the mass flow rate appear to be almost constant during this period. Therefore, the change in compressor discharge temperature is believed to have affected the change in compressor work as enthalpy of the refrigerant increases as a consequence of the temperature increase of the refrigerant at the compressor discharge.

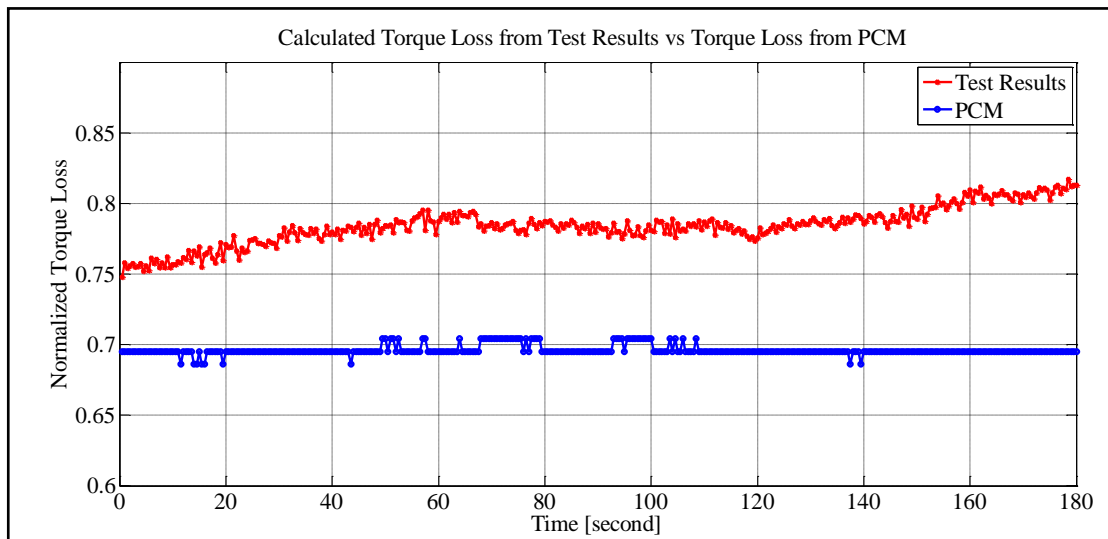


Figure 4.4. Comparison of the compressor torque loss between test results and PCM output at average of 2038rpm engine speed and 17°C outside temperature test

Compressor torque requirement is the one that is needed for compressor torque loss map calibration. Figure 4.4 shows the comparison between the calculated torque loss of the compressor from the vehicle tests and the torque loss output of the pre-calibrated torque loss map from PCM. It can be observed that the pre-calibrated torque loss map gives almost constant output around 0.7 throughout the 180 seconds period. This is an expected result since the map gives the output based on the pressure of the refrigerant at compressor discharge and compressor speed. Since engine speed and refrigerant pressure are almost constant during this period, the map gives almost constant output. On the other hand, the result of the vehicle test data changes in accordance with compressor power requirement through this period. As indicated previously, compressor power requirement increases due mostly to the refrigerant temperature increase at the compressor discharge, and compressor torque requirement shows the same behaviour because the torque requirement is calculated from the compressor power. The test results show around 0.78 unit torque loss which differs by around 10% from the PCM torque loss map output.

Figures 4.5 and 4.6 illustrate the comparison of the compressor torque loss values between the PCM output and the test results for the engine speeds of 2505 and 2926 rpm.

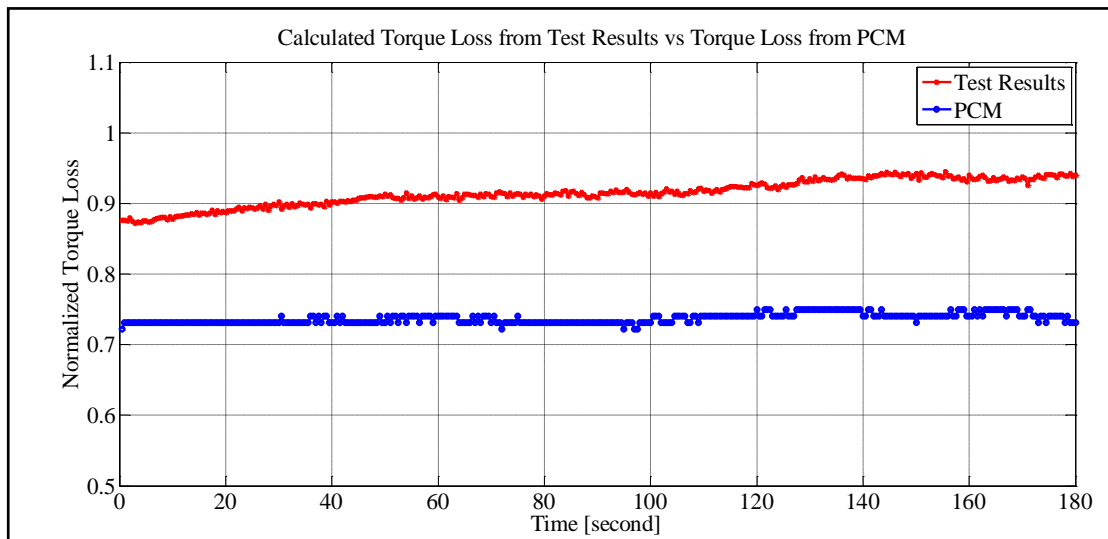


Figure 4.5. Comparison of the compressor torque loss between test results and PCM output at average of 2505 rpm engine speed and 17°C outside temperature test

It can be observed from Figure 4.5 that compressor torque loss outputs from the PCM torque loss map are almost constant through this time period as in the case of the 2038 rpm engine speed tests since the output of this map only depends on the pressure of the refrigerant at compressor exit and engine speed. Since these two variables are almost constant through the test, PCM gives nearly constant torque loss values for the compressor. On the other hand, compressor torque requirement from the test results increases slightly as time elapses. This is again mainly due to increase in the temperature of the refrigerant at the compressor discharge. The enthalpy of the refrigerant increases due to increase in refrigerant temperature at compressor exit and this change is greater than the change in enthalpy of the refrigerant at compressor suction. The mass flow rate of the refrigerant is nearly constant as the compressor suction pressure and the engine speed are almost constant during the test period. The test results show the compressor torque loss to be around 0.92 while the torque loss map output is around 0.74. Therefore, compressor torque loss calculations from the vehicle tests give approximately 20% higher results compared to PCM torque loss map output. The reason for this much of difference may be caused by the fact that torque loss map cannot reflect the real torque loss value of the compressor at every operating point since the output of the map only depends on the refrigerant pressure at compressor discharge and engine speed. It is obvious from the tests results that the temperature of the refrigerant changes continuously throughout the tests which directly

affects the enthalpy of the refrigerant and compressor power requirement. But it is not possible to show this change in the compressor torque loss map as the refrigerant pressure and the engine speed are almost constant through the test period.

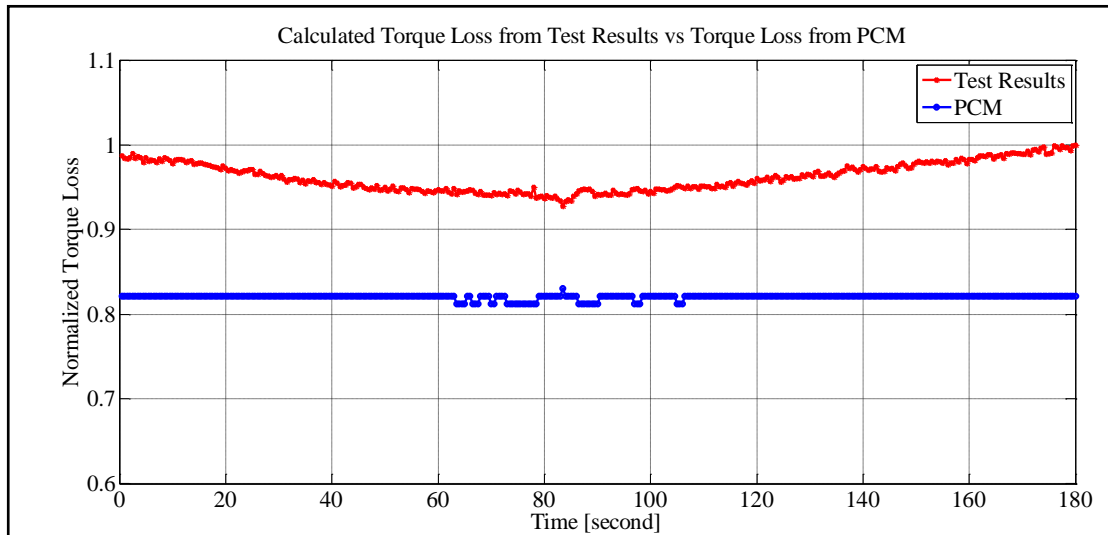


Figure 4.6. Comparison of the compressor torque loss between test results and PCM output at average of 2926 rpm engine speed and 17°C outside temperature test

Figure 4.6 shows the results for average of 2926 rpm engine speed tests. PCM torque loss map gives around 0.8 compressor torque loss while test results give around 0.96. The test results give approximately 14.5 % higher torque loss value for the compressor. The variation of the torque loss value of the compressor from the vehicle tests is due to the fact that temperature of the refrigerant changes slightly at compressor discharge during the tests so enthalpy of the refrigerant changes. This ends up with change in compressor torque loss for the vehicle tests. Since the refrigerant pressure at compressor discharge and engine speed are almost constant, the torque loss map gives nearly same outputs as in the case of previous tests.

Table 4.3 shows the average values of the analyses results with the torque loss outputs of the PCM torque loss map. The average values of the results are used to examine the change in COP, isentropic efficiency and torque loss values among the tests.

Table 4.3. Normalized average values of the test results for 17°C outside temperature tests

Normalized Engine Speed	0.67	0.83	0.97
Normalized Mass Flow Rate	0.91	0.95	0.99
Normalized Isentropic Efficiency of the Compressor	0.75	0.53	0.46
Normalized COP of the A/C system	0.55	0.40	0.34
Normalized Compressor Torque Loss From Test Results	0.78	0.92	0.96
Normalized Compressor Torque Loss From PCM	0.70	0.74	0.82
Normalized Compressor Power	0.54	0.77	0.95

When Table 4.3 is examined, it can be observed that mass flow rate of the refrigerant increases with increase in engine speed. Note that the mass flow rate is calculated as a function of the engine speed and the compressor suction pressure. The test result shows that all compressor suction pressures at different engine speeds are very close to each other since evaporator inlet temperatures differ around 1.5°C for all tests at different engine speeds. Therefore, the mass flow rate of the refrigerant is mainly a function of the engine speed throughout the tests.

Isentropic efficiency of the compressor decreases as engine speed increases according to test results. The change in isentropic efficiency is caused by change in the temperature of the refrigerant at compressor discharge. As illustrated in Table 4.2 temperature of the refrigerant increases with increasing engine speed. So, isentropic efficiency of the compressor decreases mainly due to increase in the enthalpy of the refrigerant at compressor exit when engine speed increases. The same situation applies for COP results. It can be observed that COP of the system decreases as engine speed increases. The dominant effect for this result is the increase in the temperature of the refrigerant when engine speed increases.

The increase in the mass flow rate and the enthalpy of the refrigerant indicates increase in compressor power requirement. As it can be observed from Table 4.3 that compressor power requirement increases with increasing engine speed. This result is consistent with the results for mass flow rate and the temperature of the refrigerant at compressor discharge. Since compressor power is calculated based on Equation 2.3, the increase in

both mass flow rate and enthalpy at the compressor exit causes the compressor power to increase.

The average values of the torque loss calculations from the test results show that compressor torque loss increases with increasing engine speed as in the case of compressor power. The average values of the analyses results and the PCM torque loss map outputs show increasing trend with increasing engine speed although there is a discrepancy between test results and torque loss map outputs. The maximum difference between the test results and torque loss map output is observed as 20% in the test of 2505 rpm (which corresponds to 0.83 in unit base) average engine speed.

There may be several reasons for the discrepancy between the test results and the torque loss map output. First of all, the torque loss map is calibrated with referencing to the previous projects so it just includes base calibration which has not been validated. Also, the torque loss map output depends on the refrigerant pressure at compressor discharge and engine speed. So, it may not be possible to reflect the torque loss of the compressor accurately with this calibration map since it is not possible to include the change in the torque loss of the compressor caused by the temperature change of the refrigerant either at compressor suction or discharge. Thus, the torque loss change caused by the change in the refrigerant temperature especially at the compressor exit cannot be reflected in the torque loss map which may cause wrong calculations for the compressor torque loss. Lastly, the resolution of the calibration map may affect the output. Since the number of X and Y axes are restricted due to memory constraint of PCM, it is not possible to calibrate every operating point of the compressor although data would be available for it. Thus, only limited operating points can be calibrated with this map while the other points are calculated by interpolation inside PCM. So, this may be another reason for the discrepancy between the test results and the torque loss map output. Due to all of these reasons, it is believed that the test results give more accurate torque loss values for the compressor although they may subject to some errors. The test results may include some measurement and calculation errors. Since the temperature measurements of the refrigerant are collected from the surface of the A/C pipes and some part of the pipes are located under the engine compartment, the surface of the pipes may be affected from the engine temperature although they are insulated. This has direct effect on the temperature data collected from



the A/C system. Also, there may be some measurement errors caused by measurement setup and the accuracy of the thermocouples and pressure sensor.

### 4.3. TEST RESULTS AT 11 °C OUTSIDE TEMPERATURE

Other vehicle tests are performed at three different engine speed points when ambient air temperature is around 11°C. The same procedure with the previous tests is applied for these tests also. Temperature and pressure data are collected from the A/C system by putting the vehicle at a specific gear and cruise control is activated to collect data at constant engine speed points. The average engine speed points for these tests are 1615 rpm, 2039 rpm and 2504 rpm. In this part of the report, only the torque loss comparison plots are presented since the system behavior is very similar to the previous tests. The results are given again on unit base by dividing the each parameter by the maximum value obtained among all test results presented in this study.

Table 4.4 illustrates the engine speed, the refrigerant pressure and temperature at compressor discharge and refrigerant temperature at evaporator inlet and exit.

Table 4.4. Normalized average values of the temperature and pressure data of the refrigerant from 11°C outside temperature tests

Normalized Engine Speed	0.53	0.67	0.83
Normalized Discharge Pressure	0.66	0.69	0.67
Normalized Compressor Outlet Temperature	0.41	0.51	0.56
Normalized Evaporator Inlet Temperature	0.01	0.02	0.01
Normalized Evaporator Outlet Temperature	0.04	0.04	0.04

Refrigerant pressure at compressor exit is almost constant among these tests although engine speed changes. These results are consistent with the data collected from the previous tests. When the refrigerant pressure measurements at compressor discharge are compared with the test results at 17°C which are given in Table 4.2, it can be observed that the refrigerant pressure values at compressor discharge are lower at lower ambient

temperature. Therefore, it can be said that increasing outside air temperature increases the refrigerant pressure at compressor discharge.

The temperature of the refrigerant at compressor discharge increases with increasing engine speed as in the case of previous test results although the refrigerant pressure is almost constant through the tests.

Evaporator inlet and outlet temperatures does not change so much with changing engine speed. This is a desired result as the system is designed to control the evaporator temperature at a specified temperature. Since the refrigerant absorbs heat from the cabin while passing through the evaporator and becomes superheated at evaporator outlet, its temperature increases slightly at evaporator outlet.

Figure 4.7 through 4.9 illustrates the torque loss values of the compressor from the PCM torque loss map and test results during 40 seconds for 1615 rpm, 2039 rpm and 2504 rpm engine speed points respectively.

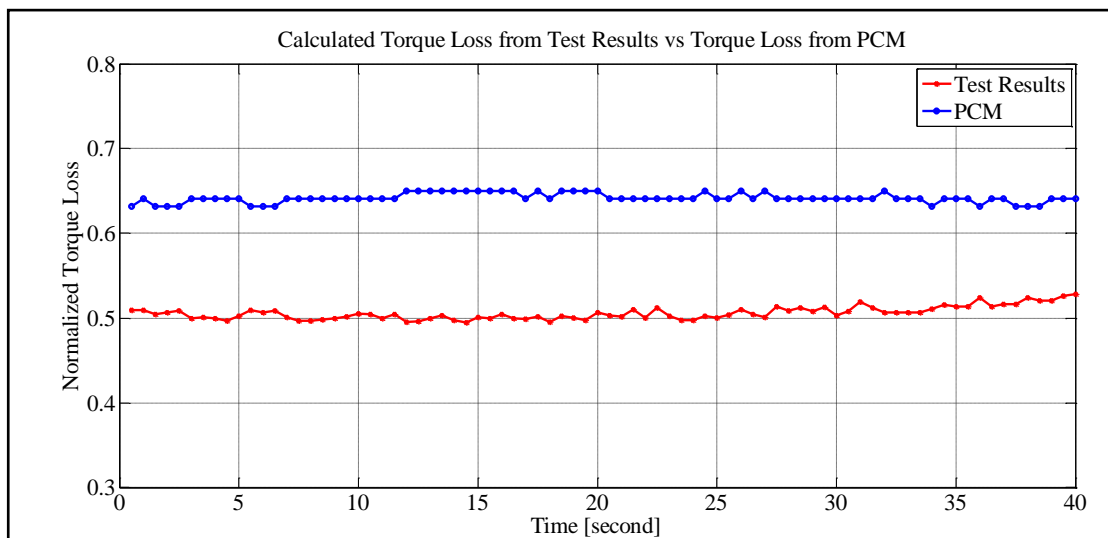


Figure 4.7. Comparison of the compressor torque loss between test results and PCM output at average of 1615 rpm engine speed and 11°C outside temperature test

Figure 4.7 shows that compressor torque loss values are calculated around 0.50 based on vehicle test results and the torque loss map outputs are around 0.64. This means

calculations from vehicle test data give approximately 20% less torque loss outputs compared to pre-calibrated torque loss map. The torque loss outputs of the calibration map is almost constant during this period since the refrigerant pressure at compressor exit and engine speed are almost constant during test periods. The torque loss outputs from the test results change slightly during the test period but as it can be observed from the figure there is no major change in the torque loss values from the beginning of 40 seconds time period.

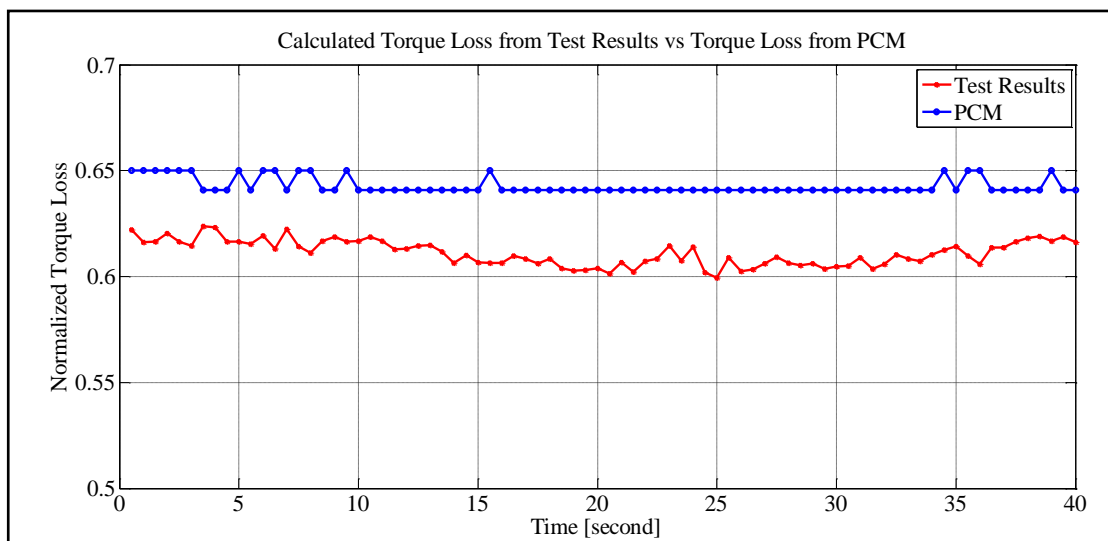


Figure 4.8. Comparison of the compressor torque loss between test results and PCM output at average of 2039 rpm engine speed and 11°C outside temperature test

The torque loss outputs for average engine speed of 2039 rpm are given in Figure 4.8. The results show that the torque loss map outputs give around 0.64 and the analyses results give around 0.61 torque loss for the compressor. This means the torque loss map outputs are approximately 5% higher than the test results.

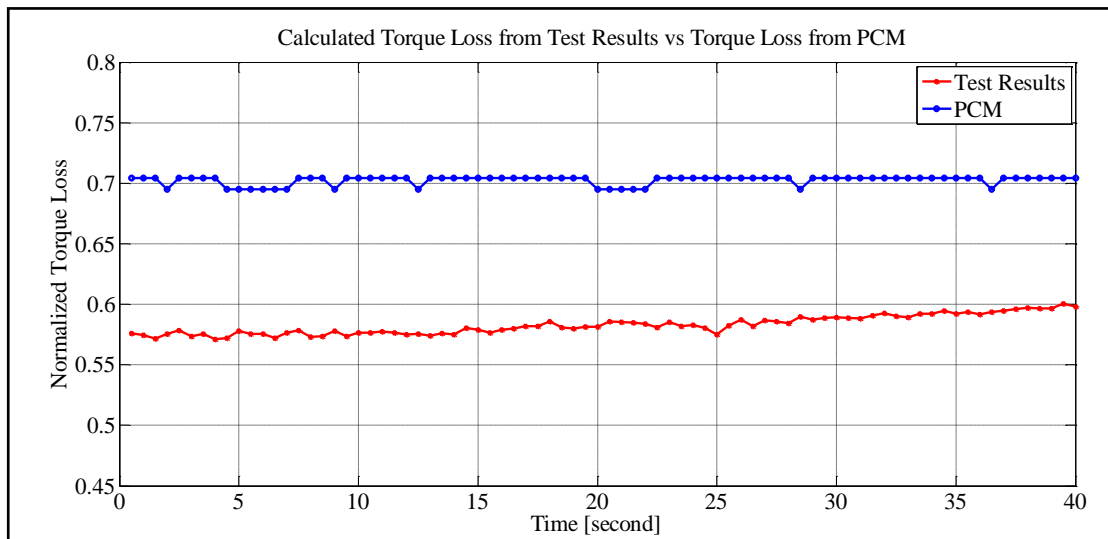


Figure 4.9. Comparison of the compressor torque loss between test results and PCM output at average of 2504 rpm engine speed and 11°C outside temperature

Comparison for the compressor torque loss values for average of 2504 rpm engine speed is presented in Figure 4.9. The torque loss map gives the maximum output at this test among three tests performed at 11°C ambient temperature. The test results for the compressor torque loss gives around 0.58 which is approximately 17% less than the torque loss map outputs. Since the refrigerant pressure and engine speed are almost constant through this period, the torque loss map gives nearly constant output. It can be observed that the compressor torque loss values from the analyses results increases slightly. This is due to the fact that the enthalpy of the refrigerant increases at compressor discharge since its temperature increases although the refrigerant pressure at compressor suction is almost constant.

The average value of the analyses results for three different engine speed points are presented in Table 4.5.

Table 4.5. Normalized average values of the test results for 11°C outside temperature tests

Normalized Engine Speed	0.53	0.67	0.83
Normalized Mass Flow Rate	0.78	0.90	0.93
Normalized Isentropic Efficiency of the Compressor	0.95	0.75	0.65
Normalized COP of the A/C system	0.98	0.73	0.64
Normalized Compressor Torque Loss From Test Results	0.51	0.61	0.58
Normalized Compressor Torque Loss From PCM	0.64	0.64	0.70
Normalized Compressor Power	0.28	0.42	0.49

It can be observed from Table 4.5 that the average values of the mass flow rate of the refrigerant increase with increasing engine speed since the refrigerant pressure are almost same among the tests at different engine speeds. So, the maximum value for the mass flow rate is observed in the tests results of maximum engine speed which is 2504 rpm (0.83 on unit base).

Isentropic efficiency of the compressor decreases with increasing engine speed since the refrigerant temperature at compressor discharge increases with increases engine speed as presented in Table 4.4. The increase in temperature causes enthalpy increase for the refrigerant so isentropic efficiency of the compressor decreases with increasing refrigerant enthalpy at compressor discharge based on Equation 2.2. It should be noted that the enthalpy of the refrigerant at compressor suction is almost constant since its pressure and temperature are almost constant at compressor inlet.

Another effect of the increasing enthalpy of the refrigerant at compressor discharge is seen as decrease in COP with increasing engine speed. It can be observed from Table 4.5 that the COP of the system decreases in accordance with increased enthalpy of the refrigerant at compressor outlet. COP of the A/C system is calculated based on Equation 2.1 and it can be observed that increase in the enthalpy of the refrigerant at compressor discharge causes COP to decrease since the temperature and pressure of the refrigerant at evaporator inlet and outlet and compressor suction are almost constant during the test periods.

The average values of the compressor power requirements show that compressor power input increases with increasing engine speed. The two effects for compressor power to increase are the increase in mass flow rate of the refrigerant and increase in the enthalpy of the refrigerant at compressor discharge with increasing engine speed.

If the average values for the compressor torque loss values are compared it can be observed that torque loss map output gives maximum of 20% higher results at average engine speed of 1615 rpm (which corresponds to 0.53 on unit base) compared to analyses results. The torque loss map outputs and the test results are in good agreement in the results of 2039 rpm engine speed (which corresponds to 0.67 on unit base). The torque loss values from the test results are approximately 5% lower compared to the torque loss map output at 2039 rpm engine speed.

#### 4.4. TEST RESULTS AT 21 °C OUTSIDE TEMPERATURE

Vehicle tests at three different engine speeds are performed when environmental air temperature is 21°C. The averages of engine speeds for these tests are 2064 rpm, 2540 rpm and 2968 rpm. Each test is performed approximately 5 minutes at constant vehicle speeds to ensure the temperature and pressure data from the A/C system are stabilized.

Table 4.6 presents the average values of the collected data on unit base. The average values are obtained by using the 60 seconds period of the tests data.

Table 4.6. Normalized average values of the temperature and pressure data of the refrigerant from 21°C outside temperature tests

Normalized Engine Speed	0.68	0.84	0.98
Normalized Discharge Pressure	0.94	0.96	0.95
Normalized Compressor Outlet Temperature	0.70	0.84	0.93
Normalized Evaporator Inlet Temperature	0.02	0.03	0.03
Normalized Evaporator Outlet Temperature	0.04	0.05	0.05

It can be observed from test results that the refrigerant pressure at compressor discharge is not a function of the engine speed as average values of the discharge pressure are nearly same among these tests. But it can be observed that the refrigerant pressure increases with increasing ambient air temperature when the values of refrigerant pressure at compressor discharge are examined for different ambient air temperatures given in Table 4.2 and 4.4. It can be easily concluded that the refrigerant pressures at compressor discharge at 21 °C ambient temperature are higher than the pressures observed at 11°C and 17 °C ambient temperature.

The refrigerant temperature at compressor discharge increases with increasing engine speed as in the case of previous test results. When the refrigerant temperature at evaporator inlet and outlet are compared with the temperature of the refrigerant at compressor discharge, it can be easily observed that compressor discharge temperature levels are much higher than evaporator temperatures as expected. Also it can be observed that refrigerant temperature increases from evaporator inlet to evaporator outlet as in the case of previous test results.

The comparison of compressor torque loss values for average engine speeds of 2064 rpm, 2540 rpm and 2968 rpm are given in Figures 4.10 to 4.12.

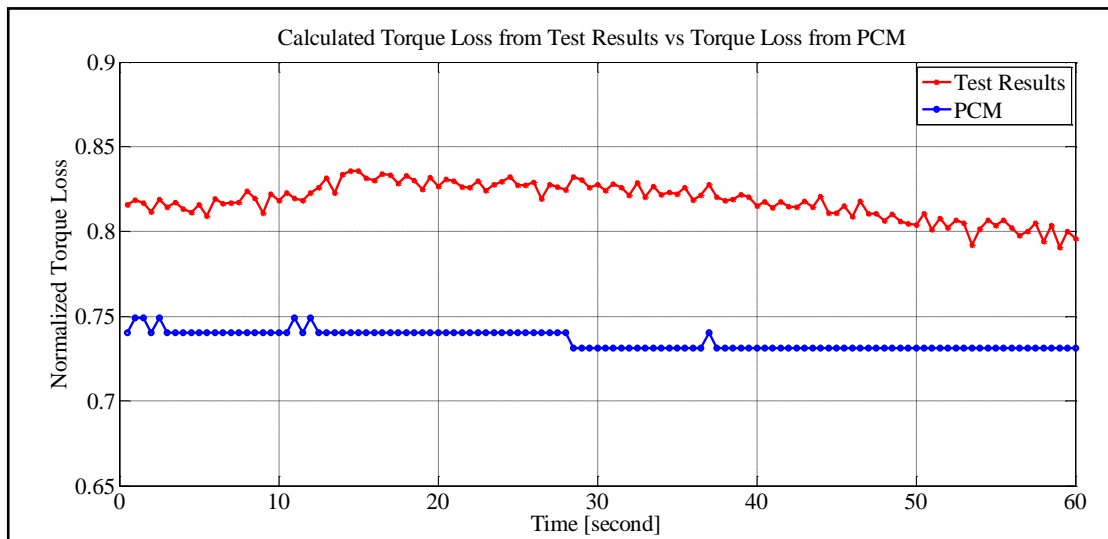


Figure 4.10. Comparison of the compressor torque loss between test results and PCM output at average of 2064 rpm engine speed and 21°C outside temperature

Figure 4.10 shows the comparison of compressor torque loss values between analysis results and the output of the pre-calibrated torque loss map for average of 2064 rpm engine speed tests. It can be observed that the output of the torque loss map gives around 0.74 and the test results show that the torque loss of the compressor is around 0.82. The test results give approximately 10 % higher torque loss values. It can be also observed from the figure that the compressor torque loss values from the test results changes slightly with respect to time. The dominant effect for this change is the change in the enthalpy of the refrigerant at compressor discharge since it is observed that mass flow rate of the refrigerant and the enthalpy of the refrigerant at compressor suction is almost constant during this period. The change in refrigerant enthalpy at compressor discharge is mainly caused by the temperature change of the refrigerant although there is small change in the pressure of the refrigerant at compressor discharge.



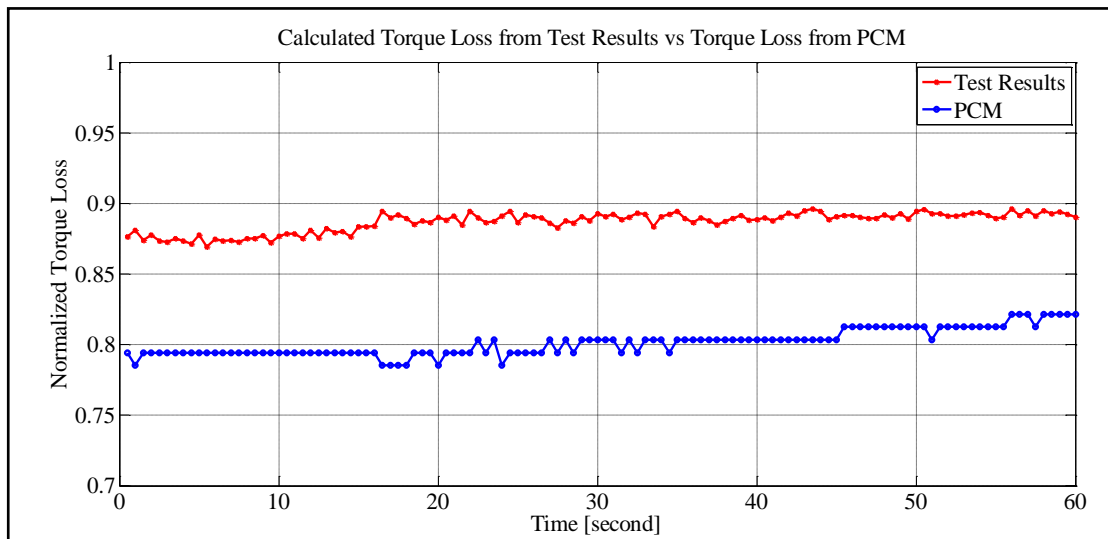


Figure 4.11. Comparison of the compressor torque loss between test results and PCM output at average of 2540 rpm engine speed and 21°C outside temperature

The torque loss comparison of the torque loss values between the test results and torque loss map output are introduced in Figure 4.11 for the average engine speed of 2540 rpm. It can be observed that compressor torque loss is calculated around 0.89 based on vehicle test data and the torque loss map output is around 0.80. The test results give approximately 11% higher compressor torque loss compared to torque loss map output.

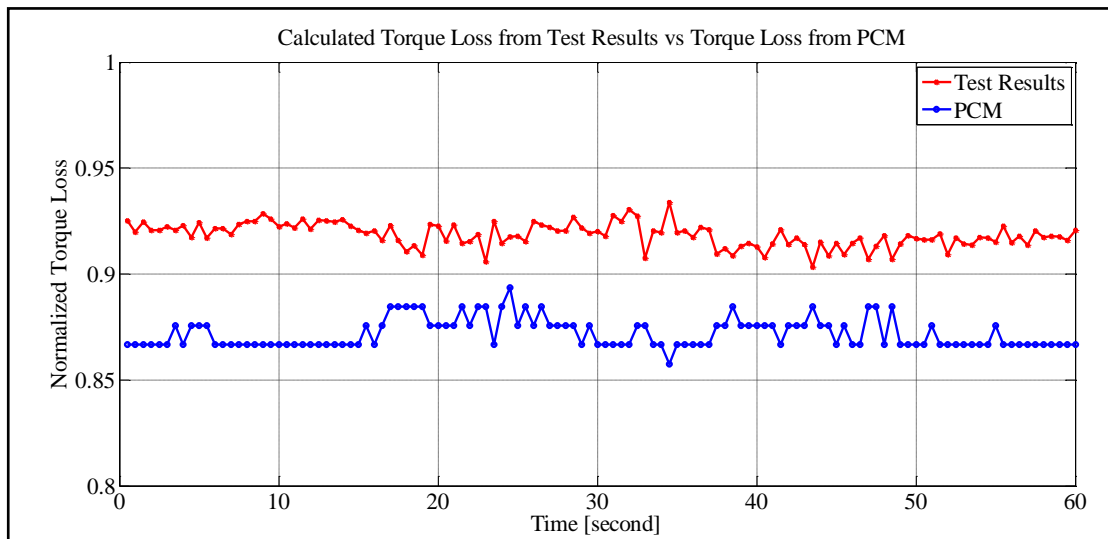


Figure 4.12. Comparison of the compressor torque loss between test results and PCM output at average of 2968 rpm engine speed and 21°C outside temperature

Figure 4.12 introduces the comparison of analyses results and torque loss map outputs for average engine speed of 2968 rpm. When the figure is examined, it can be observed that test results give higher torque loss values than the torque loss map outputs. The calculations from vehicle test data give approximately 0.92 and the pre-calibrated torque loss map gives output of around 0.87 for the compressor torque loss. The variation in the torque loss map outputs may be caused by the change in the refrigerant pressure at compressor outlet and small changes in engine speed during the test period. The test results estimate approximately 5% higher compressor torque loss compared to PCM torque loss map output.

The average values of the analyses results for mass flow rate, isentropic efficiency, COP, compressor torque loss and compressor power as well as the average values of the PCM torque loss map for three different engine speed tests are introduced in Table 4.7.

Table 4.7. Normalized average values of the test results for 21°C outside temperature tests

Normalized Engine Speed	0.68	0.84	0.98
Normalized Mass Flow Rate	0.91	0.95	1.00
Normalized Isentropic Efficiency of the Compressor	0.83	0.65	0.55
Normalized COP of the A/C system	0.51	0.40	0.34
Normalized Compressor Torque Loss From Test Results	0.82	0.89	0.92
Normalized Compressor Torque Loss From PCM	0.74	0.80	0.87
Normalized Compressor Power	0.57	0.76	0.92

The average values of the mass flow rates show that the mass flow rate increases with increasing engine speed. This trend is consistent with the output of the previous test results. Since the pressure of the refrigerant at compressor suction is almost constant and nearly same among these tests, the dominant effect for the mass flow rate of the refrigerant is engine speed.

The average values of the isentropic efficiency also show the similar trend as in the case of previous test results. The average values of isentropic efficiency of the compressor decreases with increasing engine speed as it can be observed from Table 4.7. The main reason for isentropic efficiency decrease is caused by increase in the temperature of the refrigerant at compressor discharge. The increase in the temperature of the refrigerant at compressor exit causes the enthalpy of the refrigerant to increase. Since the temperature of the refrigerant at compressor suction does not vary so much with changing engine speed, the increase in temperature of the refrigerant dominates the change in isentropic efficiency. The same situation applies for the decrease in COP with increasing engine speed.

If the average values of the compressor power requirement are examined, it is observed that power requirement of the compressor increases with increasing engine speed. Since power input to the compressor is calculated based on Equation 2.3, it depends on the mass flow rate, enthalpy of the refrigerant at compressor suction and discharge. It is obvious that both increase in mass flow rate and the enthalpy of the refrigerant at compressor discharge contribute to increase in compressor power requirement when engine speed increases.

Both the average values of the compressor torque loss from the PCM torque loss map and the test results show increasing trend with increasing engine speed although test results overestimate the torque loss of the compressor at each engine speed points compared to the torque loss map output. The maximum difference between the analyses results and the torque loss map is observed as 11% at average engine speed point of 2540 rpm (which corresponds to 0.84 on unit base) tests.

#### 4.5. TEST RESULTS AT 23 °C OUTSIDE TEMPERATURE

Last tests are performed when the ambient air temperature is around 23°C which is the hottest environment among all the vehicle tests conditions presented in this study. The tests are performed when the blower level at defrost and blower fan is at position 1 as in the case of previous tests. The average engine speeds for three different tests are 2064 rpm, 2537 rpm and 2967 rpm. The test duration for each test is approximately 4 minutes.

The average values of the engine speed, refrigerant pressure at compressor discharge, refrigerant temperature at compressor outlet, evaporator inlet and outlet are introduced in Table 4.8.

Table 4.8. Normalized average values of the temperature and pressure data of the refrigerant from 23°C outside temperature tests

Normalized Engine Speed	0.68	0.84	0.98
Normalized Discharge Pressure	0.96	0.96	0.98
Normalized Compressor Outlet Temperature	0.73	0.84	0.98
Normalized Evaporator Inlet Temperature	0.02	0.03	0.03
Normalized Evaporator Outlet Temperature	0.04	0.04	0.04

The test conditions are very similar to the tests that are performed at ambient air temperature of 21°C except that ambient temperature is approximately 2°C higher in these tests. So, it is observed that the refrigerant pressure at compressor discharge are very close to the values that are obtained from the tests at 21°C ambient temperature which are presented in Table 4.6.

The refrigerant temperature at compressor discharge shows consistent trend as in the previous tests as refrigerant temperature increases with increasing engine speed at compressor exit. There is slight increase in the refrigerant temperature from evaporator inlet to outlet as expected although evaporator inlet and outlet temperatures do not change so much with respect to engine speed.

The output of the torque loss map and test results for compressor torque loss are presented in Figures 4.13 through 4.15 for average engine speed of 2064 rpm, 2537 rpm and 2967 rpm respectively.

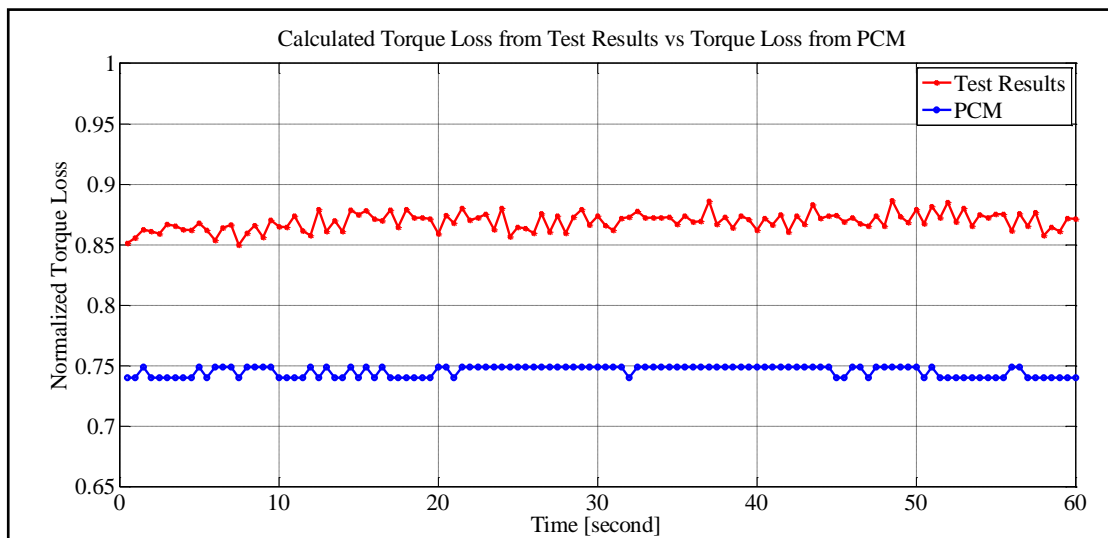


Figure 4.13. Comparison of the compressor torque loss between test results and PCM output at average of 2064 rpm engine speed and 23°C outside temperature

It can be observed from Figure 4.13 that the test results give higher compressor torque loss values for the average engine speed of 2064 rpm tests. Although torque loss map outputs are around 0.75, the test results give around 0.87 which leads approximately 16% overestimation compared to PCM torque loss map output.

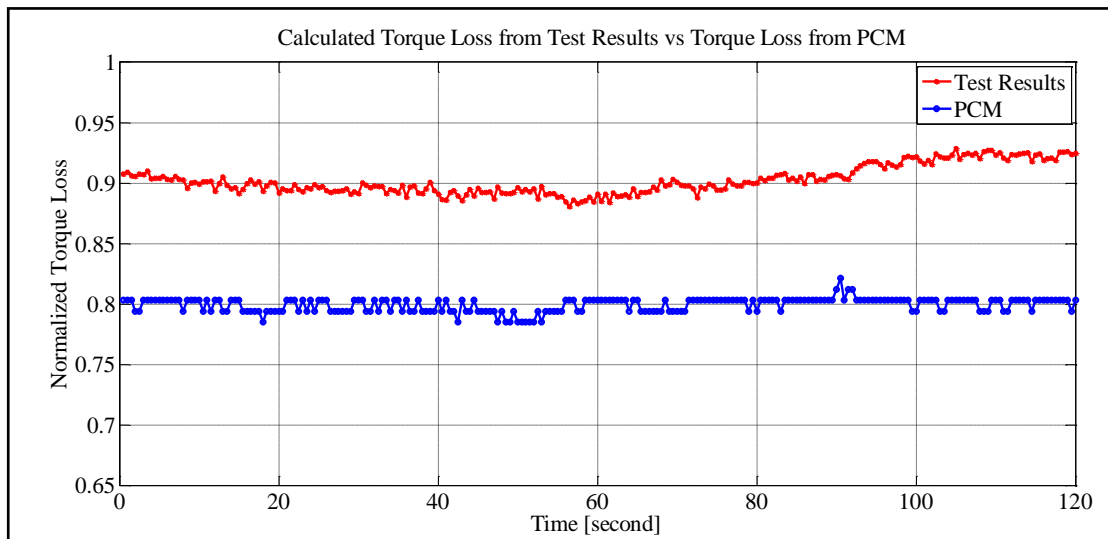


Figure 4.14. Comparison of the compressor torque loss between test results and PCM output at average of 2537 rpm engine speed and 23°C outside temperature

Compressor torque loss values from the test results and the compressor torque loss map for the average engine speed of 2537 presented in Figure 4.14. The analyses give the compressor torque loss approximately 0.90 although it is calculated around 0.8 from torque loss map. The analyses results give approximately 12% more torque loss for the compressor. It can be observed from the figure that compressor torque loss values from the test results increase slightly toward the end of the tests although torque loss map give nearly constant results. The main reason for the change in the compressor torque during the test period is caused by the change in the refrigerant temperature at compressor discharge. The change in temperature causes enthalpy of the refrigerant to change so it changes compressor torque requirement as compressor torque loss is calculated based on Equation 2.4. It should be noted that the enthalpy of the refrigerant remains almost constant along with engine speed and mass flow rate during this period so the dominant effect for the change in torque loss outputs from the analyses is the change in the enthalpy of the refrigerant at compressor discharge.

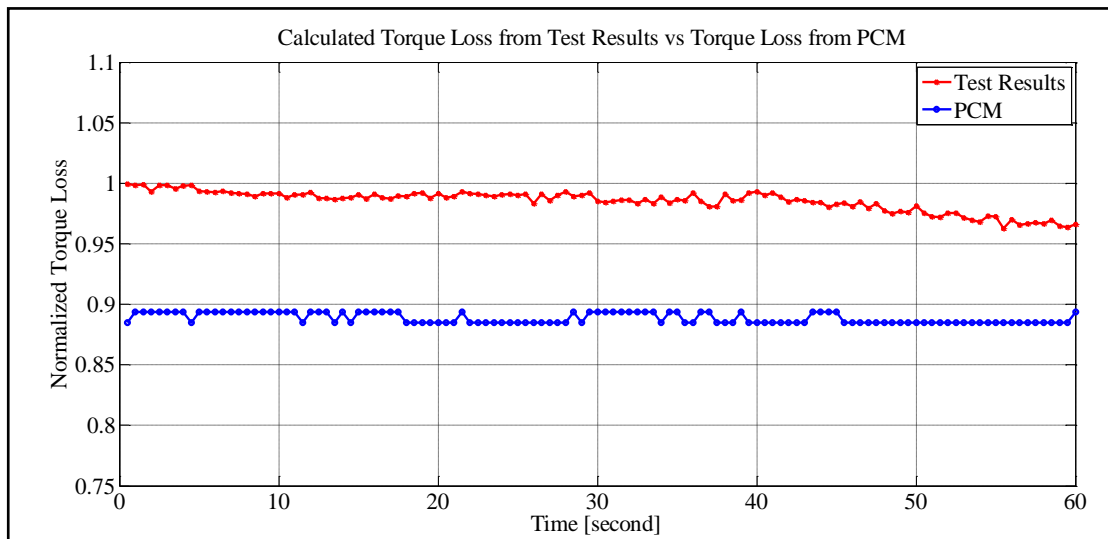


Figure 4.15. Comparison of the compressor torque loss between test results and PCM output at average of 2967 rpm engine speed and 23°C outside temperature

The last test is performed at average engine speed of 2967 rpm at 23°C ambient temperature. Figure 4.15 show the comparison of compressor torque loss outputs from the analyses results and torque loss map. The analyses give around 0.99 torque loss while the torque loss map output is around 0.89. The analyses give approximately 11% higher torque loss values compared to torque loss map output. It is observed from the figure that compressor torque loss values decreasing toward the end of the test period. When the temperature data for this test is examined, it is observed that the refrigerant temperature at compressor discharge decreases slightly toward the end of the test. This causes enthalpy decrease for the refrigerant at compressor discharge. Since enthalpy of the refrigerant at compressor suction and mass flow rate of the refrigerant are almost constant during the test, it can be said that temperature decrease of the refrigerant at compressor discharge causes the torque loss decrease.

Table 4.9 gives the average values of the test results for mass flow rate, isentropic efficiency, COP, compressor power and compressor torque loss estimations. The average values for the compressor torque loss values from PCM calibration map are also listed.

Table 4.9. Normalized average values of the test results for 21°C outside temperature tests

Normalized Engine Speed	0.68	0.84	0.98
Normalized Mass Flow Rate	0.91	0.95	0.99
Normalized Isentropic Efficiency of the Compressor	0.79	0.65	0.54
Normalized COP of the A/C system	0.47	0.38	0.31
Normalized Compressor Torque Loss From Test Results	0.87	0.90	0.99
Normalized Compressor Torque Loss From PCM	0.75	0.80	0.89
Normalized Compressor Power	0.60	0.77	0.99

The mass flow rate of the refrigerant increases with increasing engine speed as expected. Since engine speed points and the refrigerant pressure at compressor suction for these tests are very close to the tests performed at 21°C ambient temperature, mass flow rate values almost same compared to the 21°C test results.

The isentropic efficiency of the compressor and COP of the system decreases with increasing engine speed due to the fact that the temperature of the refrigerant increases at compressor discharge with increasing engine speed as it can be observed from Table 4.8. The increase in the refrigerant temperature at compressor discharge causes the enthalpy of the refrigerant to increase while the enthalpy of the refrigerant at evaporator inlet and outlet does not change so much with changing engine speed. Therefore, isentropic efficiency of the compressor and COP of the system decreases with increasing engine speed which is consistent with Equation 2.1 and 2.2.

It can be observed from Table 4.9 that required compressor power increases with increasing engine speed as in the case of all other test results. This is an expected result because mass flow rate and the enthalpy of the refrigerant increases with increasing engine speed.

When the average values of the test results for the compressor torque loss and torque loss map calibration outputs are compared, it can be easily observed that test results overestimates the compressor torque loss compared to torque loss map outputs. The



maximum difference between the analyses results and torque loss map outputs is observed as 16 % at 2064 rpm engine speed (which corresponds to 0.68 on unit base) tests.

If the entire test results presented in this study is assessed together, it can be concluded that the refrigerant pressure at compressor discharge increases with increasing environmental air temperature. Therefore, the maximum refrigerant pressure at compressor discharge occur at 23°C ambient air temperature vehicle tests and the minimum pressure values are observed at 11°C ambient temperature tests.

The vehicle tests results also show that compressor power and torque loss are strongly depend on the temperature and pressure of the refrigerant at compressor discharge. This is due to the fact that the refrigerant is superheated at compressor discharge and its enthalpy is calculated based on its temperature and pressure. When ambient air temperature increases, the pressure of the refrigerant at compressor discharge increases as indicated previously which contributes to the decrease of the compressor power since the enthalpy of the refrigerant decreases with increasing refrigerant pressure at compressor discharge. On the other hand, the increase in the temperature of the refrigerant at compressor discharge causes the enthalpy of the refrigerant to increase which leads to the increase in the compressor power. Although there is no trend among the entire test results for the temperature of the refrigerant at compressor discharge with changing ambient temperature at the same engine speed points, it can be observed from the test results that the temperature of the refrigerant generally increases with increasing ambient temperature. So, increasing ambient temperature generally causes the enthalpy of the refrigerant to increase at same engine speed points which lead to increase in compressor power. Therefore, it can be concluded that for the same engine speed points at different ambient temperatures, compressor power and torque loss values change with the mutual effect of the change in the temperature and pressure of the refrigerant at compressor discharge. Since the mass flow rate of the refrigerant is almost same for the same engine speed, this has no major effect on the compressor power and torque loss values for the same engine speed calculations.

#### 4.6. A/C COMPRESSOR TORQUE LOSS MAP CALIBRATION

The torque loss map of the A/C compressor is re-calibrated by the test results. Since all of the operating points of the map are not covered with vehicle tests, only regions where the test data are available are calibrated based on the test results.

The calibration process is performed in Hardware in the Loop (HIL) system. The HIL system includes the vehicle and engine model and PCM as hardware. Therefore, it is possible to perform calibration work without requiring a vehicle by simulating the test conditions that are performed in real world. The regions of the torque loss map that are covered in vehicle tests are re-calibrated by simply setting the engine speed and refrigerant pressure to the same values of the vehicle tests. Once the engine speed and refrigerant pressure are set to the values of vehicle tests, these regions of the map are updated based on the test results. The updated map is given in Table 4.10 where re-calibrated regions are colored in red.

Table 4.10. Normalized steady-state A/C compressor torque loss map that is re-calibrated based on test results

Y \ X	0.031	0.077	0.160	0.200	0.280	0.360	0.520	0.717	1.000
0.182	0.083	0.139	0.208	0.264	0.361	0.444	0.639	0.833	1.000
0.236	0.111	0.158	0.228	0.289	0.411	0.514	0.750	0.917	1.000
0.295	0.139	0.161	0.239	0.300	0.436	0.550	0.806	0.958	1.000
0.355	0.167	0.103	0.239	0.375	0.447	0.567	0.833	0.981	1.000
0.414	0.167	0.128	0.247	0.372	0.536	0.661	0.917	1.000	1.000
0.473	0.167	0.194	0.306	0.400	0.572	0.700	0.944	1.000	1.000
0.591	0.172	0.264	0.308	0.542	0.722	0.814	0.986	1.000	1.000
0.709	0.219	0.283	0.411	0.597	0.778	0.850	0.994	1.000	1.000
0.945	0.250	0.314	0.506	0.725	0.883	0.911	0.967	0.967	0.967

The X axis of the map depends on the refrigerant pressure at compressor discharge and the engine speed and the Y axis of the map is the engine speed.

It should be noted that the number of axis in Table 4.10 is different from the map that is used for vehicle tests which is given in Table 4.1 although the definitions of the axes are the same. It is observed from the test results that very small region of the pre-calibrated torque loss map is used for different engine speed and refrigerant discharge pressure conditions although the calculated torque loss values from the vehicle tests are different. Therefore, to be able to reflect the torque loss of the A/C compressor more accurately, it is decided to increase the axis size of the torque loss map. The number of X axis is increased from 6 to 9 and the number of Y axis is increased from 4 to 9 which are the maximum number of breakpoints for the torque loss map that PCM memory allows. In this manner, it is aimed to calculate compressor torque loss values more accurately at different engine speed and refrigerant pressure conditions by increasing the resolution of the compressor torque loss map.

It should be noted that all of the regions of the map have not been updated based on test results as it can be observed from Table 4.10. In order to calibrate the other regions of the map, therefore, more test data are required at different outside air temperature and engine speed conditions.

## 5. CONCLUSION

In this study the air conditioning (A/C) system of a commercial vehicle is investigated experimentally. The A/C system of the vehicle is instrumented with surface thermocouples to collect required temperature data for the thermodynamic analyses. The temperature and pressure data are collected from the instrumentation sensors in addition to the sensors that are already implemented to the vehicle. Vehicle tests are performed at different outside temperatures and engine speeds to collect data. The collected temperature and pressure data along with the other required data are used to perform thermodynamic analysis of the system. The test data are processed with MATLAB scripts to obtain isentropic efficiency of the compressor, coefficient of the performance (COP) of the system and compressor power and torque loss values.

The test results show that the refrigerant pressure at the compressor discharge is a strong function of environmental air temperature. The compressor discharge pressure is observed to be higher when ambient air temperature is higher. On the other hand, the compressor discharge pressure appears to show little variation with the engine speed.

It is observed from the test results that the isentropic efficiency of the compressor is strongly dependent on the engine speed when the outside air temperature is constant. The reason for the strong dependency of the isentropic efficiency on the engine speed may be explained by the test results that the compressor discharge temperature increases with the increasing engine speed while the compressor suction temperature remains little changed with the engine speed. Therefore, a higher engine speed results in lower isentropic efficiency while higher isentropic efficiency is observed at lower engine speed.

The coefficient of performance (COP) of the system also depends on the engine speed. It is observed from the test results that COP of the system decreases with increasing engine speed at the same environmental air temperature conditions. The reason for this change is also caused mainly due to increase in the temperature of the refrigerant at the compressor discharge when engine speed increases. Thus, higher COP values are observed at lower engine speed operating points.

The compressor power input is calculated at various engine speeds and refrigerant pressures. The test analyses show that the steady-state compressor power increases with increasing engine speed when the refrigerant pressure is constant. Since the pressure of the refrigerant is almost constant if the ambient air temperature does not change, the compressor work input increases with increasing engine speed as a result of the increase in the enthalpy and mass flow rate of the refrigerant.

The A/C compressor torque loss is also calculated from the compressor power by the analysis on the test data. The torque loss values obtained by analysing the test result are used to calibrate the steady-state torque loss map of the A/C compressor. The test results for the torque loss of the compressor are compared with the output of the pre-calibrated torque loss map. The results show that the maximum difference between the test results and PCM torque loss map outputs is approximately 20%. It is observed that the pre-calibrated torque loss map may give higher and lower compressor torque loss values compared to the test results. Since the pre-calibrated torque loss map just includes base calibration which is not validated specific to the used vehicle, the test results are believed to be more accurate, compared to the torque loss map outputs. Furthermore, the output of the compressor torque loss map depends only on the engine speed and the pressure of the refrigerant at compressor discharge, and thus the torque loss map does not include the effect of the temperature change of the refrigerant at compressor discharge on compressor torque loss. This constitutes another reason that the test results are thought to be more reliable compared the outputs of the torque loss map.

The steady-state torque loss map of the compressor is updated by the torque loss results from the vehicle tests. The calibration process is performed in Hardware in the Loop (HIL) rig which includes the engine and vehicle model and PCM as hardware. So, it is possible to simulate the real world test conditions in HIL rig. The compressor torque loss map is calibrated by setting the engine speed and refrigerant pressure to the values of the vehicle tests and changing the torque loss values in the map to the values that are obtained from vehicle tests. This provides calibration process without requiring any vehicle usage.

As a result of the present study, some but not all regions of the compressor torque loss map have been calibrated by the test data. More data should be collected at different engine

speeds and refrigerant pressures to calibrate the whole regions of the PCM compressor torque loss map which are not covered by the present test data.

## **6. FUTURE WORK**

The present study calibrates some regions of the torque loss map of the A/C compressor. As a future work, more tests are required at different engine speeds and refrigerant pressures to calibrate all the regions of the steady-state torque loss map of the A/C compressor.

Moreover, calibration of the transient torque loss map of the A/C compressor remains to be explored in the future. In order to study the transient torque loss, more tests should be performed to collect transient data from the A/C system at various operating conditions.

## APPENDIX A: THE DEVELOPED MATLAB SCRIPT

Table A.1. The developed Matlab script that performs the thermodynamic analyses

```

function [omg_comp, AC_trqcomp, Wcomp, COPr, QL_dot, QH_dot,
isent_eff, mdot] = AC_Cycle(); %function that calculates
required outputs
% mdot = mass flow rate [kg/s]
% h1 = enthalpy at evaporator outlet [kJ /kg]
% h2 = enthalpy at compressor outlet [kJ /kg]
% h3 = enthalpy at condenser outlet [kJ /kg]
% h4 = enthalpy at evaporator inlet - after TXV [kJ /kg]
% h2s = enthalpy at compressor outlet - if isentropic [kJ
/kg]
% AC_trqComp = Compressor torque loss [Nm]
% eff_isent = isentropic efficiency of the compressor [%]
% COPr = coefficient of performance
% QL_dot = heat absorption from refrigerated space [kW]
% QH_dot = heat rejection to warm environment [kW]
% N_eng = engine speed [rpm]
% N_comp = compressor speed [rpm]
% omg_comp = compressor speed [rad/s]
% Wcomp = compressor power [kW]
% w = compressor speed [rad/s]
% point 1: Evaporator outlet
% point 2: Compressor outlet / condenser inlet
% point 3: Condenser outlet / TXV in
% point 4: Evaporator inlet / TXV outlet
%%%%%%%%%%%%%%%%%%%%%%%%%%%%%%%%%%%%%%%%%%%%%%%%%%%%%%%%%%%%%%%%%%%%%%%%
%%%%%%%%%%%%%%%%%%%%%%%%%%%%%%%%%%%%%%%%%%%%%%%%%%%%%%%%%%%%%%%%%%%%%%%%

[Tevap_in, Tevap_mid, Tevap_out, Tcompressor_in, Plow,
Tcompressor_out, Phigh, Tcondenser_out, N_eng,
CompTrqLoss_fromPCM] = Read_TestData_To_Mat();

```



```

pulleyratio = ;

for j=1:numel(N_eng)

    N_comp(j) = N_eng(j) * pulleyratio;

    mdot(j) = mass_flow_rate(N_comp(j),Plow(j));

    if Tcompressor_in(j) >
saturation_temperatures(Plow(j))

        [v1(j),h1(j),s1(j)] = superheated_properties(
Tcompressor_in(j), Plow(j));
    else

        v1(j) = 0;
        h1(j) = 0;
        s1(j) = 0;

    end

    if Tcompressor_out(j) > saturation_temperatures(Phigh(j))

        [v2(j),h2(j),s2(j)] =
superheated_properties(Tcompressor_out(j), Phigh(j));
    else

        v2(j) = 0;
        h2(j) = 0;
        s2(j) = 0;

    end

    [psat3(j), vf3(j), vg3(j), hf3(j), hg3(j), sf3(j),
sg3(j)] = saturated_properties(Tcondenser_out(j));
    h2s(j) = isentropic_enthalpy(Phigh(j), s1(j));

```

```

    h4(j) = hf3(j);

    omg_comp(j) = (N_comp(j))*((2*pi)/60); % convert engine
speed to comp speed to rad/s
    QH_dot(j) = mdot(j)*(h2(j) - hf3(j)); %kW
    QL_dot(j) = mdot(j)*(h1(j) - h4(j)); %kW
    Wcomp(j) = mdot(j)*(h2(j) - h1(j)); %kW

    COPr(j) = QL_dot(j) / Wcomp(j);
    isent_eff(j) = 100*((h2s(j) - h1(j)) / (h2(j) - h1(j)));
% percentage
    AC_trqcomp(j) = (Wcomp(j)*1000)/omg_comp(j); %Nm

end

figure;
subplot('Position',[0.1 0.1 0.87 0.8]); %[left bottom width
height]
plot((1:length(AC_trqcomp))*0.5,AC_trqcomp,'r*-
','LineWidth',3);hold on;
plot((1:length(CompTrqLoss_fromPCM))*0.5,CompTrqLoss_fromPCM,
'bo-','LineWidth',3);
title('Calculated Torque Loss from Test Results vs Torque
Loss from PCM','FontSize',24,'FontName','Times New Roman');
set(gca,'FontSize',24,'FontName','Times New
Roman','FontWeight','Normal')
% set(gca,'XTick',0:100:1200)
% set(gca,'YTick',0:100:1500)
legend('Test Results','PCM','FontSize',24,'FontName','Times
New Roman')
xlabel('Time [second]','FontSize',24,'FontName','Times New
Roman')
ylabel('Torque Loss [Nm]','FontSize',24,'FontName','Times New
Roman')
grid on;

function [Tevap_in, Tevap_mid, Tevap_out, Tcompressor_in,
Plow, Tcompressor_out, Phigh, Tcondenser_out, N_eng,

```

```

CompTrqLoss_fromPCM] = Read_TestData_To_Mat();

load .mat

CompTrqLoss_fromPCM = AC_trqDes.signals.values; % Nm

Tevap_in = Evaporator_Inlet.signals.values; %degC

Tcompressor_in = Compressor_Suction.signals.values; %degC

Tcompressor_out = Compressor_Discharge.signals.values; %degC

Tcondenser_out = Condenser_Outlet.signals.values; %degC

Tevap_out = Evaporator_Outlet.signals.values ; %degC

Tevap_mid = AC_tEvapT.signals.values ;

Phigh = AC_pClntUsT.signals.values/10; %kPa

for k=1:numel(Tevap_in)

    Plow(k) = saturated_properties(Tevap_in(k)); %kPa

end

N_eng = Epm_nEng.signals.values; %rpm

end

function [psat,vf,vg,uf,ug,hf,hg,sf,sg] =
saturated_properties(Tsat)

load R134a_saturated.mat

```

```

T_Levels = Properties_Struct_Sat.Tsat;
[rsat,csat,vsat]= find(T_Levels'>=Tsat);

T1 = T_Levels(csat(1)-1);
T2 = T_Levels(csat(1));

psat1 = Properties_Struct_Sat.Psat(csat(1)-1);
psat2 = Properties_Struct_Sat.Psat(csat(1));
psat=psat2-(((psat2-psat1)*(T2-Tsat))/(T2-T1));

vf1 = Properties_Struct_Sat.vf(csat(1)-1);
vf2 = Properties_Struct_Sat.vf(csat(1));
vf = vf2-(((vf2-vf1)*(T2-Tsat))/(T2-T1));

vg1 = Properties_Struct_Sat.vg(csat(1)-1);
vg2 = Properties_Struct_Sat.vg(csat(1));
vg = vg2-(((vg2-vg1)*(T2-Tsat))/(T2-T1));
uf1 = Properties_Struct_Sat.uf(csat(1)-1);
uf2 = Properties_Struct_Sat.uf(csat(1));
uf = uf2-(((uf2-uf1)*(T2-Tsat))/(T2-T1));

ug1 = Properties_Struct_Sat.ug(csat(1)-1);
ug2 = Properties_Struct_Sat.ug(csat(1));
ug = ug2-(((ug2-ug1)*(T2-Tsat))/(T2-T1));

hf1 = Properties_Struct_Sat.hf(csat(1)-1);
hf2 = Properties_Struct_Sat.hf(csat(1));
hf = hf2-(((hf2-hf1)*(T2-Tsat))/(T2-T1));

hg1 = Properties_Struct_Sat.hg(csat(1)-1);
hg2 = Properties_Struct_Sat.hg(csat(1));
hg = hg2-(((hg2-hg1)*(T2-Tsat))/(T2-T1));

sf1 = Properties_Struct_Sat.sf(csat(1)-1);
sf2 = Properties_Struct_Sat.sf(csat(1));
sf = sf2-(((sf2-sf1)*(T2-Tsat))/(T2-T1));

sg1 = Properties_Struct_Sat.sg(csat(1)-1);

```

```

sg2 = Properties_Struct_Sat.sg(csat(1));
sg = sg2-(((sg2-sg1)*(T2-Tsat))/(T2-T1));

end

function [v,h,s] = superheated_properties(T,P)

if (P >= 100) && (P <= 3000) && (T <= 120)

    load R134a_superheat.mat
    Pressure_Levels = [100 140 180 220 260 300 310 312 314
316 318 320 330 340 380 420 460 500,...
        600 700 800 900 1000 1200 1400 1600 1800 2000 2200
2400 2600 2800 3000];

    if P == 100
        P1 = 100;
        P2=140;
    else
        [r,c,v]= find(Pressure_Levels>=P);
        P1 = Pressure_Levels(c(1)-1);
        P2 = Pressure_Levels(c(1));
    end

    T_Levels = Properties_Struct.(char(['Prop_' num2str(P1)
'kpa'])).T;
    [rT,cT,vT]= find(T_Levels'>=T);
    T1 = T_Levels(cT(1)-1);
    T2 = T_Levels(cT(1));

    v11 = Properties_Struct.(char(['Prop_' num2str(P1)
'kpa'])).v(cT(1)-1);
    v21 = Properties_Struct.(char(['Prop_' num2str(P2)
'kpa'])).v(cT(1)-1);
    v12 = Properties_Struct.(char(['Prop_' num2str(P1)

```

```

'kpa'])).v(cT(1));
    v22 = Properties_Struct.(char(['Prop_' num2str(P2)
'kpa'])).v(cT(1));

    h11 = Properties_Struct.(char(['Prop_' num2str(P1)
'kpa'])).h(cT(1)-1);
    h21 = Properties_Struct.(char(['Prop_' num2str(P2)
'kpa'])).h(cT(1)-1);
    h12 = Properties_Struct.(char(['Prop_' num2str(P1)
'kpa'])).h(cT(1));
    h22 = Properties_Struct.(char(['Prop_' num2str(P2)
'kpa'])).h(cT(1));

    s11 = Properties_Struct.(char(['Prop_' num2str(P1)
'kpa'])).s(cT(1)-1);
    s21 = Properties_Struct.(char(['Prop_' num2str(P2)
'kpa'])).s(cT(1)-1);
    s12 = Properties_Struct.(char(['Prop_' num2str(P1)
'kpa'])).s(cT(1));
    s22 = Properties_Struct.(char(['Prop_' num2str(P2)
'kpa'])).s(cT(1));

    v = bi_linear_interp(T1,T2,P1,P2,T,P,v11,v12,v21,v22);
    h = bi_linear_interp(T1,T2,P1,P2,T,P,h11,h12,h21,h22);
    s = bi_linear_interp(T1,T2,P1,P2,T,P,s11,s12,s21,s22);
end

end

function [h2s] = isentropic_enthalpy(P,s)

if (P>=100) && (P<=3000)

load R134a_superheat.mat
    Pressure_Levels = [100 140 180 220 260 300 310 312 314
316 318 320 330 340 380 420 460 500,...

```

```

        600 700 800 900 1000 1200 1400 1600 1800 2000 2200 2400
2600 2800 3000];

[r,c,v]= find(Pressure_Levels>P);
P1 = Pressure_Levels(c(1)-1);
P2 = Pressure_Levels(c(1));

s_Levels1 = Properties_Struct.(char(['Prop_' num2str(P1)
'kpa'])).s;
[rs1,cs1,vs1]= find(s_Levels1'>s);
s1_1 = s_Levels1(cs1(1)-1);
s1_2 = s_Levels1(cs1(1));

s_Levels2 = Properties_Struct.(char(['Prop_' num2str(P2)
'kpa'])).s;
[rs2,cs2,vs2]= find(s_Levels2'>s);
s2_1 = s_Levels2(cs2(1)-1);
s2_2 = s_Levels2(cs2(1));

h11 = Properties_Struct.(char(['Prop_' num2str(P1)
'kpa'])).h(cs1(1)-1);
h21 = Properties_Struct.(char(['Prop_' num2str(P2)
'kpa'])).h(cs2(1)-1);
h12 = Properties_Struct.(char(['Prop_' num2str(P1)
'kpa'])).h(cs1(1));
h22 = Properties_Struct.(char(['Prop_' num2str(P2)
'kpa'])).h(cs2(1));

h2s_int1 = h12-(((h12-h11)*(s1_2-s))/(s1_2-s1_1));
h2s_int2 = h22-(((h22-h21)*(s2_2-s))/(s2_2-s2_1));

if P == P1
    if s == s1_1
        h2s = h11;
    else
        h2s = h2s_int1;
    end
end

```

```
elseif P == P2
    if s == s2_1
        h2s = h21;
    else
        h2s = h2s_int2;
    end
else
    h2s = h2s_int2 - (((P2-P)*(h2s_int2 - h2s_int1))/(P2-
P1));

end
end
end
```



## REFERENCES

1. Summers Motors LTD., “Vehicle Air Conditioning and Servicing,”  
[http://www.summersmotors.co.uk/air\\_con.htm](http://www.summersmotors.co.uk/air_con.htm) [retrieved January 2013].
2. Visteon, “Variable Swashplate Compressor, ”  
[http://www.visteon.com/products/climate/compressor\\_variable.html](http://www.visteon.com/products/climate/compressor_variable.html) [retrieved December 2012].
3. Accurate Technologies, “Data Acquisition Modules, EDAQ Datasheet,”  
<http://www.accuratetechnologies.com/images/stories/productdatasheets/edaq%20web.pdf> [retrieved January 2013].
4. Accurate Technologies, “Data Acquisition, Vision Hub,”  
<http://www.accuratetechnologies.com/content/view/261/258/lang,en/> [retrieved January 2013].
5. Accurate Technologies, “CAN Bus Interfaces, Kvaser Products,”  
[http://www.accuratetechnologies.com/images/stories/product-datasheets/k\\_leaflight.pdf](http://www.accuratetechnologies.com/images/stories/product-datasheets/k_leaflight.pdf) [retrieved January 2013].

## REFERENCES NOT CITED

Tian, C., Liao, Y., Li, X., "A Mathematical Model of Variable Displacement Swash Plate Compressor for Automotive Air Conditioning System", *International Journal of Refrigeration*, pp. 270-280, 2006.

Kamar, H.M., Senawi, M.Y., Kamsah, N., "Computerized Simulation of Automotive Air-Conditioning System: Development of Mathematical Model and Its Validation", *International Journal of Computer Science Issues*, Vol.9, pp. 23-34, 2012.

Gordon, J., "Cooling System: Variable Displacement A/C Compressor", *Motor Age*, pp. 54-56, 2005.

"*Format for Theses*", The Institute of Graduate Studies in Science and Engineering, Yeditepe University Press, Istanbul, 2012.

Çengel Y. A. and M. A. Boles, *Thermodynamics: An Engineering Approach*, Fifth Edition, McGraw-Hill, 2006.

Incropera F. P., D. P. DeWitt, T. L. Bergman and A.S. Lavine, *Fundamentals of Heat and Mass Transfer*, Fifth Edition, WILEY, 2007.

The National Institute of Standard and Technology (NIST), "Thermophysical Properties of Fluid Systems," <http://webbook.nist.gov/chemistry/fluid/> [retrieved December 2013].

Delphi, "Air Conditioning Compressors," [http://delphi.com/pdf/contact/brochures/Delphi\\_Compressors.pdf](http://delphi.com/pdf/contact/brochures/Delphi_Compressors.pdf) [retrieved December 2012].

MATLAB, "MATLAB Documentation Center", <http://www.mathworks.com/help/matlab/> [retrieved January 2012]